

PREPARED FOR SUBMISSION TO JHEP

AUGUST 17, 2021

## Analytic structure of the Gap in Holographic superconductivity

---

Yoon-Seok Choun,<sup>a</sup> Wenhe Cai,<sup>b</sup> Sang-Jin Sin<sup>a</sup>

<sup>a</sup>*Department of Physics, Hanyang University, Seoul 04763, Korea*

<sup>b</sup>*Department of Physics, Shanghai University, Shanghai 200444, China*

*E-mail:* [youchoun@gmail.com](mailto:youchoun@gmail.com), [whcai@shu.edu.cn](mailto:whcai@shu.edu.cn), [sangjin.sin@gmail.com](mailto:sangjin.sin@gmail.com)

ABSTRACT: We analytically calculate physical observables of holographic superconductor including the critical temperature and the condensation as functions of  $\rho$ ,  $T$ ,  $\Delta$ , which are density, temperature and the scaling dimension of the Cooper pair operator respectively. In two spatial dimension, e.g, the critical temperature has the power law dependence on the coupling,  $T_c \sim (g\rho)^{1/2}$ , which can be much higher than the exponential suppression in the BCS theory,  $T_c \sim \exp(-C/g)$  for small  $g$ .

KEYWORDS: Superconductivity, Holography, AdS-CFT Correspondence

---

## Contents

<b>1</b>	<b>Introduction and Summary</b>	<b>2</b>
<b>2</b>	<b>Set up</b>	<b>5</b>
<b>3</b>	<b>Critical temperature <math>T_c</math></b>	<b>6</b>
<b>4</b>	<b>The condensation <math>\langle \mathcal{O}_\Delta \rangle</math></b>	<b>7</b>
4.1	$\langle \mathcal{O}_\Delta \rangle$ near critical temperature	7
4.2	$\langle \mathcal{O}_\Delta \rangle$ near zero temperature	8
<b>5</b>	<b>The AC Conductivity in 2+1 near the zero temperature: AdS<sub>4</sub> analysis</b>	<b>11</b>
5.1	AC conductivity for $\Delta = 1, 2$	11
5.2	The Conductivity Gap	13
5.3	The Resonant Frequencies	15
<b>6</b>	<b>Discussion</b>	<b>16</b>
<b>A</b>	<b>Holographic superconductors with AdS<sub>4</sub></b>	<b>18</b>
A.1	Near the critical temperature:	18
A.1.1	Computation of $T_c$ by applying matrix algorithm and Pincherle's Theorem	18
A.1.2	An analytic solution of $g \frac{\langle \mathcal{O}_\Delta \rangle}{T_c^\Delta}$	23
A.2	Condensate near the zero temperature	25
A.2.1	Analytic calculation of $g \frac{1}{\Delta} \frac{\langle \mathcal{O}_\Delta \rangle^{\frac{1}{\Delta}}}{T_c}$ at $1/2 < \Delta < 3$	26
A.2.2	Analytic calculation of $g \frac{1}{\Delta} \frac{\langle \mathcal{O}_\Delta \rangle^{\frac{1}{\Delta}}}{T_c}$ at $\Delta = 3/2$	30
A.3	Maxwell perturbations and the conductivity at near the zero temperature	31
A.4	Expression for the schrödinger wave equation of the conductivity at near the zero temperature	34
<b>B</b>	<b>Holographic superconductors with AdS<sub>5</sub></b>	<b>40</b>
B.1	Near the critical temperature	40
B.1.1	Computation of $T_c$ by applying matrix algorithm and Pincherle's Theorem	40
B.1.2	The analytic solution of $g \frac{\langle \mathcal{O}_\Delta \rangle}{T_c^\Delta}$	43
B.2	Condensate at near the zero temperature	44
B.2.1	Analytic calculation of $g \frac{1}{\Delta} \frac{\langle \mathcal{O}_\Delta \rangle^{\frac{1}{\Delta}}}{T_c}$ at $1 < \Delta < 4$	44
B.2.2	Analytic calculation of $g \frac{1}{\Delta} \frac{\langle \mathcal{O}_\Delta \rangle^{\frac{1}{\Delta}}}{T_c}$ at $\Delta = 2$	46

---

# 1 Introduction and Summary

In BCS theory of the superconductivity, the critical temperature is exponentially suppressed as a function of the 4-fermion coupling  $g_4$  in  $g_4\psi^\dagger\psi^\dagger\psi\psi$ , and the density of the state at the Fermi energy,  $N(0)$ , is  $N(0) \sim \rho^{1/3}$  so that  $T_c \sim e^{-1/(g_4\rho^{1/3})}$ , which explains why  $T_c$  of the conventional superconductor is so small for electron-phonon coupling.

Recent progress in the holographic superconductivity for the strong coupling regime, based on the gauge gravity duality [1–3], made remarkable progress, but similar analysis for holographic superconductors[4–6] has not been reported so far. In this paper, we will show that for the holographic superconductor in 2 spacial dimension, the  $T_c$  has power law dependence on the coupling  $g$  so that  $T_c \sim (\rho g)^{1/2}$  which is characteristically different from the BCS result. We will argue that the 4 fermion coupling  $g_4$  and the holographic minimal coupling  $g$  are dual to each other. Since the bulk coupling  $g$  is expected to be small(large) when the boundary fermions couples strongly(weakly), the result suggests that holographic superconductivity(HSC) can provide much higher  $T_c$  than BCS case, regardless of the microscopic mechanism of HSC. See the FIG. 1.

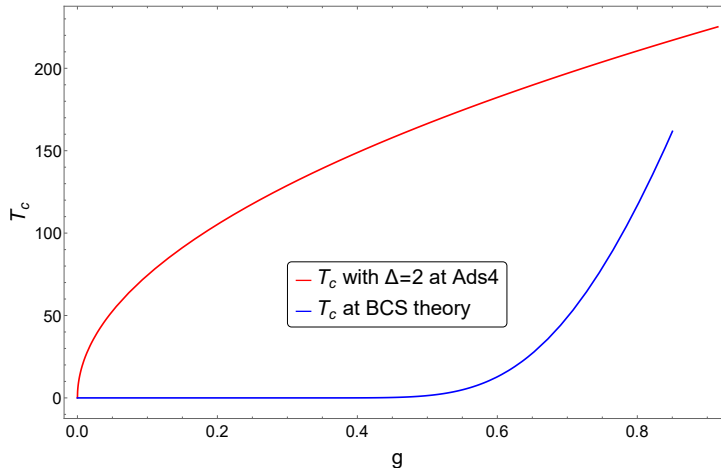


**Figure 1:**  $T_c$  vs the coupling: blue line is for BCS and red is for the holographic theory.

On the other hand, shortly after the ground breaking works on HSC [4, 5], the authors of ref. [7] calculated interesting physical observables of the superconductivity for a few values of  $\Delta$ , the conformal weight of the Cooper pair operator,  $\mathcal{O}_\Delta$ . They calculated numerically  $T_c, \langle \mathcal{O}_\Delta \rangle, \sigma(\omega), \omega_g, \omega_i, n_s$ , which are the critical temperature, the condensation of the Cooper pair operator, the AC conductivity, the gap in the AC conductivity, the resonance frequencies at which  $\sigma(\omega)$  blows up, and the density of the cooper pairs respectively. The observables' dependence on  $\Delta$  is interesting because  $\Delta$  involves the anomalous dimension which depends on the interaction's strength as well as on the repulsiveness or attractiveness.

In an interesting paper [8], the authors tried to reproduce the results using analytic method and got the results which agree with those of ref. [7] partially. In this paper,

we reconsider the problem and got the results which agree with the numerical results of ref. [7] in significant detail. Since the details are rather long and cumbersome, we first summarize our results here.

The first quantity is the the Cooper pair condensation  $\langle \mathcal{O}_\Delta \rangle$  as an analytic function of  $\Delta$ , which is plotted in FIG. 2 where we compared our results (real colored lines) with those of ref. [7] (a few red dotted data ) and [8] (black broken line). Noticed that the condensation does not change much for a region around  $\Delta = 2$  and slowly increasing as  $\Delta \rightarrow 3$ . Our analytic formula reproduces the values of of ref. [7] near  $\Delta = 2$  and gives a finite value of the condensation near  $\Delta = 3$  unlike ref. [8]. Notice also that the condensation is almost independent of  $T$  and  $\Delta$  over  $3/2 < \Delta < 3$  region. Interestingly, we will see that the flatness of the graph over the region  $3/2 < \Delta < 3$  comes as a consequence of the remarkable cancellation of singularities of two functions at  $\Delta = 3/2$ . Similar result holds in three spatial dimension as well as in two dimension.

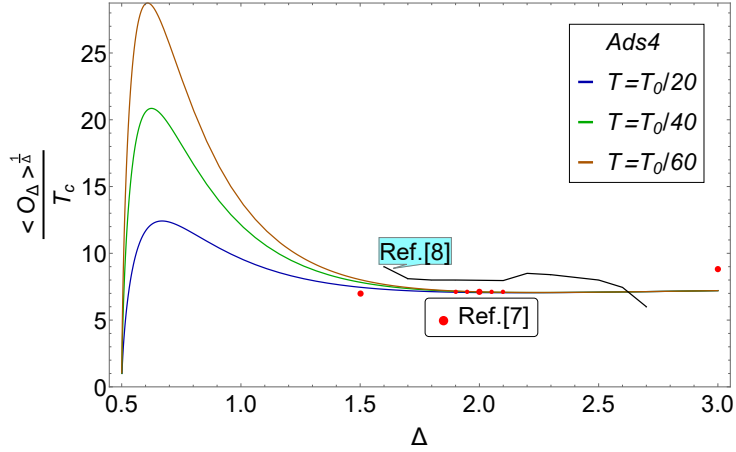


**Figure 2:**  $\langle \mathcal{O}_\Delta \rangle^{\frac{1}{\Delta}} / T_c$  vs  $\Delta$  for  $d = 3$ . Smooth colored lines are our results. Here,  $T_0 = \rho^{\frac{1}{2}}$  with  $g = 1$ . At  $\Delta = 1$ ,  $\langle \mathcal{O}_\Delta \rangle \sim (T/T_c)^{-1/3}$ . At  $\Delta = 3/2$ ,  $\langle \mathcal{O}_\Delta \rangle \sim (\ln(T_c/T))^{1/4}$ . For large  $\Delta > 3$ , the graph does not saturate to a constant but increases slowly.

Our results for  $T_c$  and  $\langle \mathcal{O}_\Delta \rangle$  for both near  $T = T_c$  and  $T = 0$  are summarized in the Table I.

AdS $_{d+1}$	$T_c \sim (g\rho)^{1/(d-1)} (\Delta - \frac{d-2}{2})^{-1/6}$
$T \approx T_c$	$\langle \mathcal{O}_\Delta \rangle \sim l^{-\Delta} g^{\gamma_g} \sqrt{1 - \frac{T}{T_c}}$ for $\frac{d-2}{2} < \Delta < d$
$T \approx 0$	$\langle \mathcal{O}_\Delta \rangle \sim l^{-\Delta} g^{\gamma_g} (\frac{T_c}{T})^{\gamma_1}$ if $\frac{d-2}{2} < \Delta \ll \frac{d}{2}$ $\langle \mathcal{O}_\Delta \rangle \sim l^{-\Delta} g^{\gamma_g} (\ln \frac{T_c}{T})^{\gamma_2}$ if $\Delta = \frac{d}{2}$ $\langle \mathcal{O}_\Delta \rangle \sim l^{-\Delta} g^{\gamma_g}$ if $\frac{d}{2} \ll \Delta < d$

**Table 1:**  $T_c$  and  $\langle \mathcal{O}_\Delta \rangle$  near  $T = T_c$  and  $T = 0$ . Here,  $\gamma_g = \frac{\Delta-(d-1)}{d-1}$ ,  $\gamma_1 = \frac{\Delta(d-2\Delta)}{(d-2+2\Delta)}$  and  $\gamma_2 = \frac{1}{2(d-1)}$  respectively, and  $l = \rho^{-\frac{1}{d-1}}$  is the distance scale given by the density  $\rho$ .

The third interesting quantity is  $\omega_g$ , the gap in the optical (AC) conductivity. Our results for the  $\omega_g$  is summarized in the Table II, which are plotted in FIG. 3. Notice

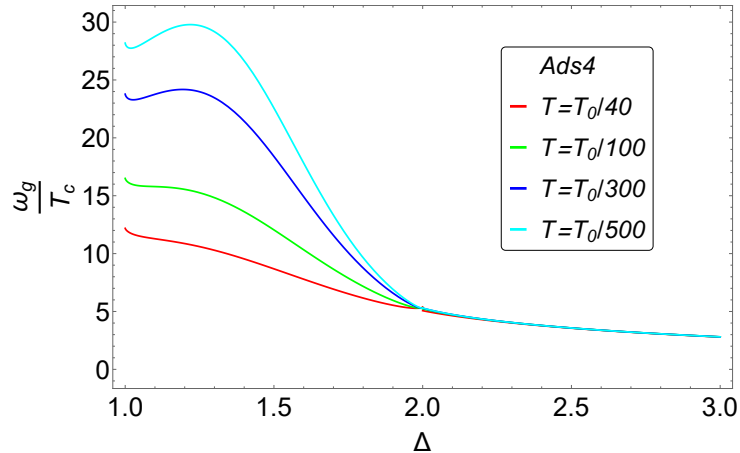


**Figure 3:**  $\omega_g/T_c$  vs  $\Delta$  for  $d = 3$ . Here,  $T_0 = (g\rho)^{\frac{1}{2}}$ . For  $\Delta > 3$ , it decreases slowly.

$\omega_g/T_c = c_1 X^\Delta \left(\frac{T_c}{T}\right)^{\Delta-1}$ , for $1 \leq \Delta \ll \frac{3}{2}$
$\omega_g/T_c = c_2 \frac{X^{3/2} \left(\frac{T_c}{T}\right)^{1/2}}{\ln(X \frac{T_c}{T})}$ , for $\Delta = \frac{3}{2}$
$\omega_g/T_c = c_3 X^{3-\Delta} \left(\frac{T_c}{T}\right)^{2-\Delta}$ for $\frac{3}{2} \ll \Delta < 2$
$\omega_g/T_c = c_4 X$ for $2 \leq \Delta \leq 3$

**Table 2:**  $\omega_g/T_c$  at  $T \approx 0$ . Here,  $X = \frac{g^{1/\Delta} \langle \mathcal{O}_\Delta \rangle^{1/\Delta}}{T_c}$ ,  $c_1 = \left(\frac{3z_0}{4\pi}\right)^{\Delta-1} \left(1 - \left(\frac{\Delta}{3-\Delta} z_0^{3/2-\Delta}\right)^2\right)$ ,  $c_2 = \frac{7}{10}$ ,  $c_3 = \left(\frac{3z_0}{4\pi}\right)^{2-\Delta} \frac{\sqrt{\pi} \Gamma\left(\frac{3+\Delta}{2+\Delta}\right) \csc\left(\frac{\pi}{2\Delta}\right)}{\Delta^{3/\Delta} \Gamma\left(\frac{\Delta}{2}\right) \Gamma\left(\frac{3}{2\Delta}\right) \Gamma\left(1+\frac{1}{\Delta}\right)} \left(1 - \left(\frac{\Delta}{3-\Delta} z_0^{\Delta-3/2}\right)^2\right)$  and  $c_4 = \frac{1.1}{\text{Li}(\Delta^{1.2})}$  with  $\text{Li}(x)$  the logarithmic integral function and  $z_0$  is a constant that is given by  $\Delta$ .

that  $\omega_g/T_c$  has the slightly decreasing tendency as a function of  $\Delta$  instead of the slowly increasing behavior of ref. [7]. So there is a small mismatch between the two.

The fourth quantity we calculated is the superfluid density  $n_s$ , which appears as the residue of the pole in the imaginary part of the optical conductivity at  $\omega = 0$ . We obtained it as an analytic function of  $\Delta$  given below,

$$\frac{n_s}{T_c} = \frac{2\pi \Delta \csc\left(\frac{\pi}{2\Delta}\right)}{(2\Delta)^{1/\Delta} \left(\Gamma\left(\frac{1}{2\Delta}\right)\right)^2} \frac{g^{1/\Delta} \langle \mathcal{O}_\Delta \rangle^{1/\Delta}}{T_c}, \quad (1.1)$$

which is plotted in FIG. 4. For this quantity, our results agree with the numerical result of ref. [7] for all the data points given there: See FIG. 4. The rest of the main text is a sketch of the proofs of above results and the details are described in the appendix.

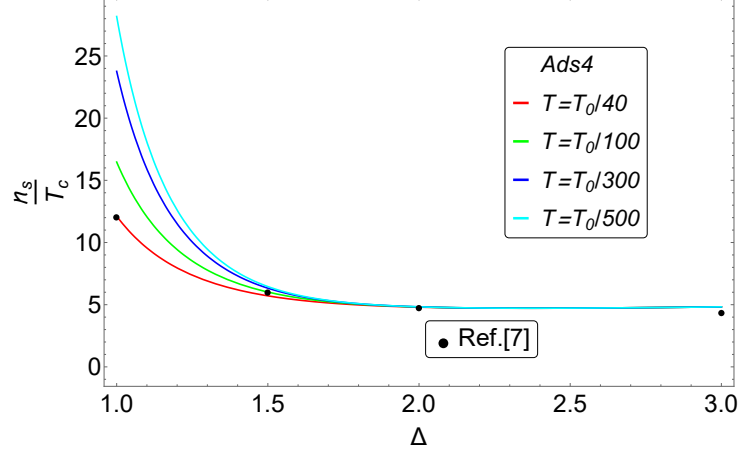


**Figure 4:**  $n_s/T_c$  vs  $\Delta$  for  $d = 3$ . Colored real lines are plots of our analytic results while the black points are numerical data of ref. [7]. Notice that it is almost independent of  $T$  and  $\Delta$  over the region  $2 \leq \Delta \leq 3$

## 2 Set up

We start with the action [4],

$$S = \int d^{d+1}x \sqrt{-|g|} \left( -\frac{1}{4} F_{\mu\nu}^2 - |D_\mu \Phi|^2 - m^2 |\Phi|^2 \right), \quad (2.1)$$

where  $|g| = \det g_{ij}$ ,  $D_\mu \Phi = \partial_\mu \Phi - ig A_\mu \Phi$  and  $F = dA$ . Following the ref.[4], we use the fixed metric of  $\text{AdS}_{d+1}$  blackhole,

$$ds^2 = -f(r)dt^2 + \frac{dr^2}{f(r)} + r^2 d\vec{x}^2, \quad f(r) = r^2 \left( 1 - \frac{r_h^d}{r^d} \right). \quad (2.2)$$

The AdS radius is set to be 1 and  $r_h$  is the radius of the horizon. The Hawking temperature is  $T = \frac{d}{4\pi} r_h$ . In the coordinate  $z = r_h/r$ , the field equations are

$$\begin{aligned} \frac{d^2 \Psi}{dz^2} - \frac{d-1+z^d}{z(1-z^d)} \frac{d\Psi}{dz} + \left( \frac{g^2 \Phi^2}{r_h^2 (1-z^d)^2} - \frac{m^2}{z^2 (1-z^d)} \right) \Psi &= 0, \\ \frac{d^2 \Phi}{dz^2} - \frac{d-3}{z} \frac{d\Phi}{dz} - \frac{2g^2 \Psi^2}{z^2 (1-z^d)} \Phi &= 0. \end{aligned} \quad (2.3)$$

Here,  $\Psi(z)$  is the scalar field and  $\Phi(z)$  is an electrostatic scalar potential  $A_t$ . Near the boundary  $z = 0$ , we have

$$\begin{aligned} \Psi(z) &= z^{\Delta_-} \Psi^{(-)}(z) + z^{\Delta_+} \Psi^{(+)}(z), \\ \Phi(z) &= \mu - (\rho/r_h^{d-2}) z^{d-2} + \dots \end{aligned} \quad (2.4)$$

where  $\Delta_\pm = d/2 \pm \sqrt{(d/2)^2 + m^2}$ ,  $\mu$  is the chemical potential and  $\rho$  is the charge density. By  $\Delta$  we mean  $\Delta_+$ .

We examine the range  $\frac{d-2}{2} < \Delta < d$  only, because the regime  $0 < \Delta < \frac{d-2}{2}$  is not physical. Notice also that  $\Delta = d/2$  is the value for which  $\Delta_+ = \Delta_-$  and  $\Delta = d$  is the value where  $m^2 = 0$ . We request the boundary conditions at the horizon  $z = 1$ :  $\Phi(1) = 0$  and the finiteness of  $\Psi(1)$ . Then the condensate of the Cooper pair operator  $\mathcal{O}_\Delta$  dual to the field  $\Psi$  is given by  $\langle \mathcal{O}_\Delta \rangle = \lim_{r \rightarrow \infty} \sqrt{2} r^\Delta \Psi(r)$  under the assumption that the source is zero.

### 3 Critical temperature $T_c$

At  $T = T_c$ ,  $\Psi = 0$ , and Eq.(2.3) is integrated [8] to give

$$\Phi(z) = \lambda_d r_c (1 - z^{d-2}) \text{ with } \lambda_d = \rho / r_c^{d-1}, \quad (3.1)$$

where  $r_c$  is the horizon radius at  $T_c$ . As  $T \rightarrow T_c$ , the field equation of  $\Psi$  becomes

$$-\frac{d^2 \Psi}{dz^2} + \frac{d-1+z^d}{z(1-z^d)} \frac{d\Psi}{dz} + \frac{m^2}{z^2(1-z^d)} \Psi = \frac{\lambda_{g,d}^2 (1-z^{d-2})^2}{(1-z^d)^2} \Psi \quad (3.2)$$

where  $\lambda_{g,d} = g\lambda_d$ . Our result for the critical temperature is given by

$$T_c = \frac{d}{4\pi} \left( \frac{g\rho}{\lambda_{g,d}} \right)^{\frac{1}{d-1}}, \quad (3.3)$$

which is a part of the first line of table 1. Details of deriving this result is in the appendix. For  $\Delta = 1$  and 2 in  $\text{AdS}_4$ , we have  $T_c/(g^{1/2}\sqrt{\rho}) = 0.2256$  and 0.1184 respectively. If we set our coupling  $g = 1$ , these are in good agreement with the numerical data of [4] confirming the validity of our method.

Notice that in the BCS theory,  $k_B T_c = 1.13 \omega_c e^{-\frac{1}{g_4 N(0)}}$ , where  $N(0)$  denotes the electron density at the Fermi surface, and  $\omega_c$  is the Debye cutoff. In the holographic superconductor, however, the eq.(3.3) shows that dependence of  $T_c$  on  $g$  is by power law. In order to compare the two, we argue that the boundary 4-fermion coupling  $g_4$  in  $g_4 \chi^\dagger \chi^\dagger \chi \chi$  is in fact dual to the bulk coupling term  $|g\Phi A_t|^2$  in the HSC. For this, there is no rigorous mapping between the two at this moment. However, we can intuitively understand it as follows. The complex bulk field  $\Phi$  is dual to the fermion bilinear  $\chi\chi$  of the boundary and similarly  $\Phi^*$  is dual to  $\chi^\dagger \chi^\dagger$ . Therefore  $|g\Phi A_t|^2$  is dual to the boundary term  $g_4 \chi^\dagger \chi^\dagger \chi \chi$ . Since the holographic duality is also the strong-weak duality, we expect that the bulk coupling  $g$  should be small for large boundary coupling  $g_4$ . Indeed, for large bulk coupling it is known that the result of holographic calculation resembles the semi-classical behavior of the quantum theory [9] without much fuzziness. Therefore the HSC theory with small coupling  $g$  can be regarded as the dual of strong coupling superconductivity in the boundary theory whose dynamics is not available directly. Then a holographic superconductor model with weak  $g$  can produce much higher  $T_c$  than BCS type superconductor with weak  $g_4$ , as one can see in figure 1.

To find the  $\Delta$ -dependence of the  $T_c$ , we first calculate  $\lambda_{g,d}$ . The procedures are rather involved both analytically and numerically. Here, we only display the singularity structure of the calculated data of  $\lambda_{g,d}$  leaving the details to the appendices [A.1.1](#) and [B.1.1](#):

$$\begin{aligned}\lambda_{g,3} &= 4.09 (\Delta - 1/2)^{1/3} P_3(\Delta), \\ \lambda_{g,4} &= 0.59 (\Delta - 1)^{1/2} P_4(\Delta).\end{aligned}\tag{3.4}$$

Here, we used the Pincherle's Theorem with matrix-eigenvalue algorithm[10]. Notice that the variational method used in [8] is not applicable near the singularity  $\Delta = (d - 2)/2$ . The explicit form of  $P_{3,4}(\Delta)$  and details of the derivations can be found in sections [A.1](#), [B.1](#) of supplementary material. It is important to notice that above analytic expression reveals us the singularity of  $T_c$  at  $\Delta = (d - 2)/2$ :

$$T_c \sim (\Delta - (d - 2)/2)^{-1/6}, \text{ for both } d = 3, 4.\tag{3.5}$$

The divergence of the critical temperature at some  $\Delta$  is a subtle but interesting phenomena. It is important in general theories, because it indicates that there are operators whose condensation give singularly high critical temperature of the superconductivity. However, for the holographic theory, we need  $\Delta = 1/2$  for 2+1, or  $\Delta = 1$  for 3+1 dimension, which does not seem to be practical.

## 4 The condensation $\langle \mathcal{O}_\Delta \rangle$

### 4.1 $\langle \mathcal{O}_\Delta \rangle$ near critical temperature

Next, we consider condensate near  $T = T_c$ . The result is given by

$$\frac{g \langle \mathcal{O}_\Delta \rangle}{T_c^\Delta} \approx \mathcal{M}_d \sqrt{1 - T/T_c},\tag{4.1}$$

with  $\mathcal{M}_d = (d-2) (4\pi/d)^\Delta \sqrt{(d-1)/\mathcal{C}_d}$ . The square root temperature dependence is typical of a mean field theory [4, 8, 11]. Our main interest here is the  $\Delta$  dependence of the  $\mathcal{M}_d$ , especially the singular dependence through  $\mathcal{C}_d$  whose values for some particular value of  $\Delta$  was obtained before: for  $\Delta = 1$  in  $d = 3$ , we have  $\mathcal{M}_3 = 8.367$  which is in good agreement with the  $\mathcal{M}_3 = 9.3$  [4]. For  $\Delta = 2$ , we have  $\mathcal{M}_3 = 117.4$  which roughly agrees with the results  $\mathcal{M}_3 = 119$  of ref. [12] and  $\mathcal{M}_3 = 144$  of ref. [4]. We obtained the analytic results for general  $\mathcal{M}_d$  and  $\mathcal{C}_d$ . Since they are rather lengthy we presented it in the appendix. See eq.(A.34), eq.(A.35), Eq.(B.26) and Eq.(B.27). For large  $\Delta$ ,  $\mathcal{C}_d \sim \Delta^{-6}$ , while it has a simple pole singularity  $\mathcal{C}_d \sim (\Delta - \frac{d-2}{2})^{-1}$  leading to the vanishing of  $\langle \mathcal{O}_\Delta \rangle / T_c^\Delta$  as one can see from the eq. (4.1). What happens to  $\langle \mathcal{O}_\Delta \rangle \sim T_c^\Delta (\mathcal{C}_d)^{-1/2}$ , where the divergence of  $T_c$  collide with the vanishing of  $(\mathcal{C}_d)^{-1/2}$  at  $\Delta = (d - 2)/2$ . The former can not overcome the latter unless  $\Delta > 3$ , which is different from the result of ref. [8]. We conclude that we do not have a singular dependence of the condensation anywhere for the s-wave holographic superconductivity. See the FIG. 13 of the appendix.

## 4.2 $\langle \mathcal{O}_\Delta \rangle$ near zero temperature

We can simplify Eq.(2.3) in  $T \rightarrow 0$  limit by defining

$$\Psi(z) = (\langle \mathcal{O}_\Delta \rangle / \sqrt{2} r_h^\Delta) z^\Delta F(z). \quad (4.2)$$

The equations of motion for  $F$  near the  $T_c$  becomes

$$\begin{aligned} \frac{d^2 F}{dz^2} - \frac{2\Delta + 1 - d}{z} \frac{dF}{dz} + \frac{g^2 \Phi^2}{r_h^2} F &= 0, \\ \frac{d^2 \Phi}{dz^2} - \frac{d-3}{z} \frac{d\Phi}{dz} - \frac{g^2 \langle \mathcal{O}_\Delta \rangle^2}{r_h^{2\Delta}} z^{2(\Delta-1)} F^2 \Phi &= 0. \end{aligned} \quad (4.3)$$

The boundary condition (BC) we should use are the Dirichlet condition of  $F$  and  $\Phi$  at  $z = 0$ ,

$$\frac{d\Phi(0)}{dz^{d-2}} = -\frac{\rho}{r_h^{d-2}}, \quad \frac{dF(0)}{dz} = 1, \quad (4.4)$$

and the horizon regularity conditions at  $z = 1$ ,

$$\Phi(1) = 0, \quad 3 \frac{dF(1)}{dz} + \Delta^2 F(1) = 0. \quad (4.5)$$

One should notice that  $F(0) = 1$  is not a BC but the normalization of  $\langle \mathcal{O}_\Delta \rangle$  in eq. (4.2), which we regard as a parameter to be determined.

We use  $X$  to denote  $g^{\frac{1}{\Delta}} \frac{\langle \mathcal{O}_\Delta \rangle^{\frac{1}{\Delta}}}{T_c}$  which appears often. Then,  $X$  satisfies

$$X^{2(d-1)} = G_d^{2(d-1)} (\alpha_d + \beta_d \tau_d^{d-2\Delta} X^{d-2\Delta}) \quad (4.6)$$

$$\text{where } G_d = \frac{4\pi \Delta^{1/\Delta}}{d} \left( \frac{-2^{1+\nu} \lambda_{g,d}}{\Gamma(-\nu)} \right)^{\frac{1}{d-1}} \quad (4.7)$$

$$\alpha_d = -\frac{\sqrt{\pi} \Gamma\left(\frac{d-2\Delta}{2\Delta}\right) \Gamma\left(\frac{1}{\Delta}\right) \Gamma\left(\frac{d-1}{\Delta}\right)}{8\Delta^2 \Gamma\left(\frac{d+\Delta}{2\Delta}\right)} \quad (4.8)$$

$$\beta_d = \frac{\nu\pi(d-\Delta)^2 \csc(\nu\pi)}{2\Delta^3(d-2\Delta)}. \quad (4.9)$$

with  $\nu = \frac{d-2}{2\Delta}$  and  $\tau_d = \frac{d}{4\pi \Delta^{1/\Delta}} \frac{T_c}{T}$ . For derivation of this result, see the appendix A.2. We can get the solution of Eq.(A.60) according to the regimes of  $\Delta$ :

$$X = G_d^{\frac{2(d-1)}{d-2+2\Delta}} \beta_d^{\frac{1}{d-2+2\Delta}} \tau_d^{\frac{d-2\Delta}{d-2+2\Delta}} \text{ for } (d-2)/2 < \Delta < d/2:$$

$$X = G_d \alpha_d^{\frac{1}{2(d-1)}} \text{ for } d/2 < \Delta < d. \text{ Especially, for } \Delta = \frac{d}{2}$$

$$X^{2(d-1)} = G_d^{2(d-1)} (\rho_d + \sigma_d \ln(\tau_d X)) \quad (4.10)$$

where  $\rho_d = \frac{\sigma_d}{d} \left( 5 - \frac{2}{d-2} - \pi \cot\left(\frac{2\pi}{d}\right) - 2\psi\left(\frac{2}{d}\right) - \log(4) \right)$  and  $\sigma_d = \frac{\pi(d-2)\csc\left(\frac{2\pi}{d}\right)}{d^2}$ . Here,  $\psi(z)$  is the digamma function. Details are available in appendix A.2.2 and B.2.2. Numerical results tell us that  $\rho_3 \approx 0.8$ ,  $\rho_4 \approx 0.64$  and  $\sigma_3 \approx 0.4 \approx \sigma_4$ . Therefore, eq.(4.10) becomes

$$\begin{aligned} X &\approx 6.76 \left( 1 + 0.45 \ln\left(\frac{T_c}{T}\right) \right)^{1/4} && \text{for AdS}_4 \\ X &\approx 4.9 \left( 1 + 0.57 \ln\left(\frac{T_c}{T}\right) \right)^{1/6} && \text{for AdS}_5. \end{aligned} \quad (4.11)$$

We can first test our result with known results: For  $\Delta = 1$  and  $T = 0.1T_c$ , our analytic expression with  $g = 1$  gives  $\langle \mathcal{O}_1 \rangle / T_c \approx 12.65$ , which is comparable to the numerical result 10.8 of ref. [4]. Our result, however, is different from that of ref. [8] except at  $\Delta = 1$ .

It is important to notice that the temperature dependence of the condensation is very different depending on the regime of  $\Delta$ . It diverges as  $T \rightarrow 0$  for  $\Delta < \frac{d}{2}$ , but it has little dependence on  $T$  in  $d/2 < \Delta < d$ . These results explain the numerical features of ref. [4].

Notice that there are presence of singularities at  $\Delta = d/2$  in both  $\alpha_d$  and  $\beta_d$ . Surprisingly, however, it turns out that there is no singularity in  $X$ . To understand this, notice that the behaviors of  $\alpha_d$  near  $\Delta = d/2$  is

$$\lim_{\Delta \rightarrow d/2} \alpha_d = \frac{(d-2)\pi \csc\left(\frac{2\pi}{d}\right)}{2d^2} \frac{1}{\Delta - d/2}, \quad (4.12)$$

which is exactly the same as the behavior of  $-\beta_d$  near  $\Delta = d/2$ . Therefore, the singularity of  $X$  of eq.(A.60) disappears because at  $\Delta = d/2$ ,  $X^{d-2\Delta} = 1$  and  $\alpha_d + \beta_d$  is finite. Such cancellation of two singularities was rather unexpected.

In ref. [7], it was numerically noticed that  $X$  is almost constant over the region  $d/2 < \Delta < d$ . To understand this phenomena, we plot  $\alpha_3$ ,  $\beta_3$  and  $G_3$  as function of  $\Delta$  in the FIG. 5. In fact, one can show that for  $\Delta \gg \frac{3}{2}$ ,

$$\alpha_d = \frac{\Delta}{4(d-1)d} + \frac{1 - 3\gamma_E - \psi(1/2)}{8(d-1)} + \dots, \quad (4.13)$$

so that for  $d = 3$ ,  $\alpha_3 = \frac{\Delta}{24} + 0.077$ . Notice that  $\alpha_d$  is flat over the relevant regime because the linear term grows with tiny slope.  $\beta_3$ , after vanishing at  $\Delta = 3$ , saturate to 0 rapidly like  $\sim -1/(4\Delta^2)$ . In addition,  $G_3$  moves slowly in the FIG. 5. All these collaborate with the cancellation of the singularity at  $\Delta = 3/2$ , to make the flatness of  $X$  in  $\Delta$  in the regime. Completely parallel reasoning works for  $d = 4$ . It would be very interesting to see if this is only for s-wave case or it continue to be so for  $p$ - and  $d$ -wave case as well. We will leave this as a future work. Fig. 6 is the plot of the results given in Eq.(A.60) for  $d = 3, 4$ . The solid lines are for  $d = 3$ , and the dashed lines are for  $d = 4$ . The condensation is  $\sim 7$  at  $3/2 < \Delta < 3$  for AdS<sub>4</sub>, and  $\sim 5$  at  $2 < \Delta < 4$  for AdS<sub>5</sub>. These are in good agreement with numerical results of ref. [7].

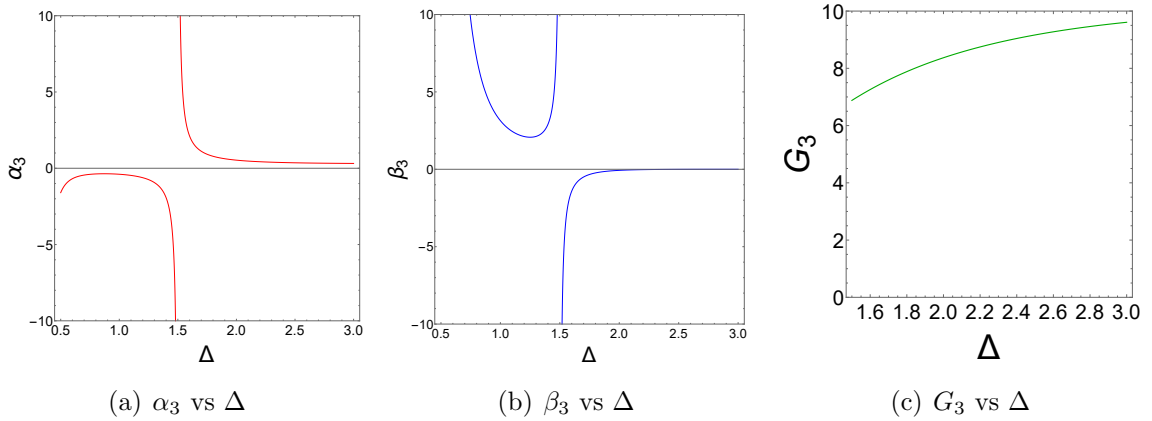


**Figure 5:** Plots of  $\alpha_3$ ,  $\beta_3$  and  $G_3$  in eq.(A.61) over  $1/2 < \Delta < 3$ .

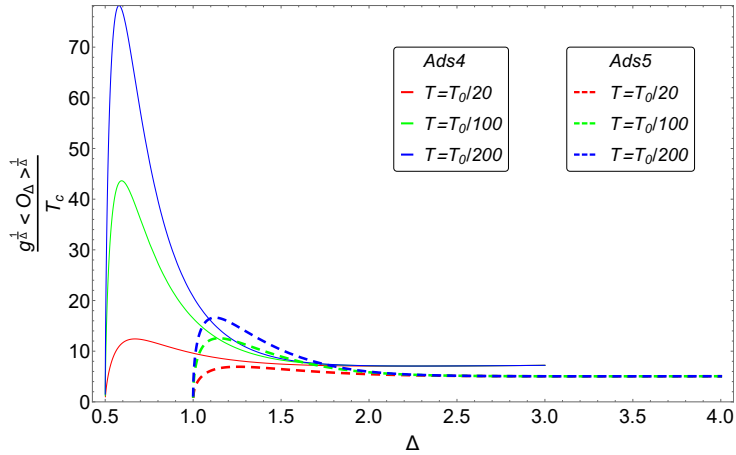


**Figure 6:**  $g^{\frac{1}{2}} \frac{(O_\Delta)^{\frac{1}{\Delta}}}{T_c}$  vs  $\Delta$  near  $T = 0$ . Here,  $T_0 = (g\rho)^{\frac{1}{2}}$ . Notice the flatness and the  $T$ -independence over  $\frac{d}{2} < \Delta < d$ .

A remark is in order to explain why analytic formulae in  $G_d$ ,  $\alpha_d$  and  $\beta_d$  were possible in spite of the fact that the differential equations in the black hole background are not of hypergeometric type, as we can see from Eq.(2.3). The simplification happens near  $T = 0$ , where the higher order singularity at the horizon disappears as we can see from Eq.(4.4): there is only one regular singularity at  $z = 0$  and the order of the singularity is independent of  $d$  so that the differential equations reduces to hypergeometric type. Details are available in appendix A.2.1, A.2.2, B.2.1 and B.2.2.

## 5 The AC Conductivity in 2+1 near the zero temperature: AdS<sub>4</sub> analysis

### 5.1 AC conductivity for $\Delta = 1, 2$

The Maxwell equation for the planar wave solution with zero spatial momentum and frequency  $\omega$  is

$$r_+^2(1-z^3)^2 \frac{d^2 A_x}{dz^2} - 3r_+^2 z^2(1-z^3) \frac{dA_x}{dz} + (\omega^2 - V(z)) A_x = 0, \quad (5.1)$$

where  $A_x$  is the perturbing electromagnetic potential and

$$V(z) = \frac{g^2 \langle \mathcal{O}_\Delta \rangle^2}{r_+^{2\Delta-2}} (1-z^3) z^{2\Delta-2} F(z)^2,$$

with  $F$  defined as before. To request the ingoing boundary conditions at the horizon,  $z = 1$ , we introduce  $G(z)$  by  $A_x(z) = (1-z^3)^{-\frac{i}{3}\hat{\omega}} G(z)$  where  $\hat{\omega} = \omega/r_+$ . Then the wave equation Eq.(5.1) reads

$$(1-z^3) \frac{d^2 G}{dz^2} - 3 \left(1 - \frac{2i\hat{\omega}}{3}\right) z^2 \frac{dG}{dz} + \left( \frac{\hat{\omega}^2(1+z)(1+z^2)}{1+z+z^2} + 2i\hat{\omega}z - \frac{g^2 \langle \mathcal{O}_\Delta \rangle^2}{r_+^{2\Delta}} z^{2\Delta-2} F^2(z) \right) G = 0 \quad (5.2)$$

If the asymptotic behaviour of the Maxwell field at large  $r$  is given by

$$A_x = A_x^{(0)} + \frac{A_x^{(1)}}{r} + \dots, \quad (5.3)$$

then the conductivity is given by

$$\sigma(\omega) = \frac{1}{i\omega} \frac{A_x^{(1)}}{A_x^{(0)}} = \frac{1}{i\hat{\omega}} \frac{dG(0)}{G(0)}. \quad (5.4)$$

Near the  $T = 0$ , the equation Eq.(5.2) is simplified to

$$\frac{d^2 G}{dz^2} + \left( \hat{\omega}^2 - \frac{g^2 \langle \mathcal{O}_\Delta \rangle^2}{r_+^{2\Delta}} z^{2\Delta-2} F(z)^2 \right) G = 0. \quad (5.5)$$

For  $\Delta = 1$ ,  $F(z) \approx 1$  so that the solution of Eq.(5.5) is

$$G(z) = \exp\left(iz\sqrt{\hat{\omega}^2 - \frac{g^2 \langle \mathcal{O}_1 \rangle^2}{r_+^2}}\right) + R \exp\left(-iz\sqrt{\hat{\omega}^2 - \frac{g^2 \langle \mathcal{O}_1 \rangle^2}{r_+^2}}\right)$$

Here,  $R$  is a constant called reflection coefficient. Taking the zero temperature limit  $T \rightarrow 0$  is equivalent to sending the horizon to infinity. Then the in-falling boundary condition corresponds to  $R = 0$ . Then it gives the conductivities:

$$\sigma(\omega) = \frac{\sqrt{\omega^2 - g^2 \langle \mathcal{O}_1 \rangle^2}}{\omega}, \quad (5.6)$$

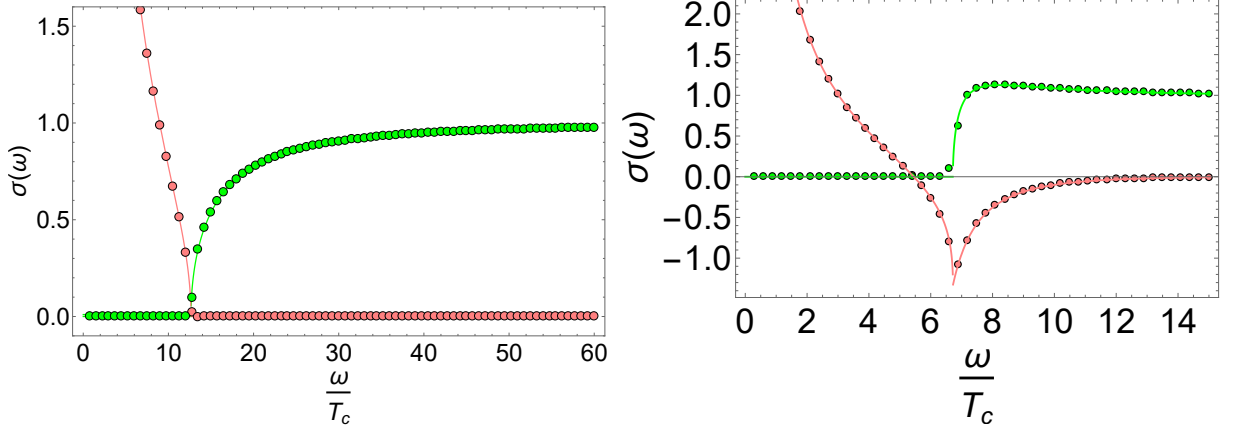
which is consistent with the result of ref. [4]. See Figure 7(a). Similarly, for  $\Delta = 2$ , we can obtain the conductivity given as follow,

$$\sigma(\omega) = \frac{3i\sqrt{g\langle\mathcal{O}_2\rangle}}{\sqrt{2\omega}} \frac{\Gamma\left(\frac{1}{36}\left(27 - \sqrt{337} - 16i\sqrt{P(\omega)}\right)\right)}{\Gamma\left(\frac{1}{36}\left(9 - \sqrt{337} - 16i\sqrt{P(\omega)}\right)\right)} \frac{\Gamma\left(\frac{1}{36}\left(27 + \sqrt{337} - 16i\sqrt{P(\omega)}\right)\right)}{\Gamma\left(\frac{1}{36}\left(9 + \sqrt{337} - 16i\sqrt{P(\omega)}\right)\right)} \quad (5.7)$$

where

$$P(\omega) = \frac{9}{8} \frac{\omega^2}{g\langle\mathcal{O}_2\rangle} - 1$$

This result fits the numerical data almost exactly as one can see in Figure 7(b). For derivation of these results, see the appendix A.3. The boundary conditions at the horizon



(a)  $\sigma(\omega)$  vs  $\omega/T_c$  at  $T/T_c = 0.1$  and  $\Delta = 1$

(b)  $\sigma(\omega)$  vs  $\omega/T_c$  at  $T/T_c = 0.1$  and  $\Delta = 2$ .

**Figure 7:** (a) pink colored curve for  $\text{Im}[\sigma(\omega)]$  and green colored one for  $\text{Re}[\sigma(\omega)]$  are analytic results of Eq.(5.6). Dot points are numerical results of Eq.(5.2). (b) pink colored curve for  $\text{Im}[\sigma(\omega)]$  and green colored one for  $\text{Re}[\sigma(\omega)]$  are analytic results of Eq.(5.7). Dot points are numerical results of Eq.(5.2).

are [13]

$$G(1) = 1, \quad \lim_{z \rightarrow 1} (1 - z^3)^{-\frac{i}{3}\hat{\omega}} G'(z) = 0.$$

To evaluate the conductivities at low frequency, it is enough to obtain  $G(z)$  up to first order in  $\omega$ ,

$$G(z) = G_0(z) + \omega G_1(z) + \mathcal{O}(\omega^2). \quad (5.8)$$

Inserting this into Eq.(5.2),  $G_0(z)$  and  $G_1(z)$  satisfy

$$(1 - z^3)G_0'' - 3z^2G_0' - \Delta^2 b^2 \Delta z^{2\Delta-2} F(z)^2 G_0 = 0, \quad (5.9)$$

$$(1 - z^3)G_1'' - 3z^2G_1' - \Delta^2 b^2 \Delta z^{2\Delta-2} F(z)^2 G_1 = -2iz(zG_0' + G_0). \quad (5.10)$$

where  $b^\Delta = \frac{g\langle\mathcal{O}_\Delta\rangle}{\Delta r_+^\Delta}$ . Near the  $T = 0$  we can simplify two coupled equations Eq.(5.9) and Eq.(5.10) as

$$G_0'' - \Delta^2 b^2 \Delta z^{2\Delta-2} G_0 = 0, \quad (5.11)$$

$$G_1'' - \Delta^2 b^2 \Delta z^{2\Delta-2} G_1 = -2izG_0. \quad (5.12)$$

The solution of Eq.(5.4) is given in Eq.(1.1). Here,  $n_s$  is the coefficient of the pole in the imaginary part  $\text{Im}\sigma(\omega) \sim n_s/\omega$  as  $\omega \rightarrow 0$ . For derivation of these results, see the appendix A.3. For the  $\Delta$  values other than 1 or 2, there is no analytic result available at this moment.

## 5.2 The Conductivity Gap

Now we begin to discuss the resonant frequencies. The Eq.(5.1) takes the form of a Schrödinger equation with energy  $\omega$ :

$$-\frac{d^2 A_x}{dr_\star^2} + V(r_\star)A_x = \omega^2 A_x, \quad (5.13)$$

where,  $V(r_\star)$  is re-expression of  $V(z) = \frac{g^2 \langle \mathcal{O}_\Delta \rangle^2}{r_+^{2\Delta-2}} (1-z^3)z^{2\Delta-2} F(z)^2$  in terms of the tortoise coordinate  $r_\star$ ,

$$r_\star = \int \frac{dr}{f(r)} = \frac{1}{6r_+} \left[ \ln \frac{(1-z)^3}{1-z^3} - 2\sqrt{3} \tan^{-1} \frac{\sqrt{3}z}{2+z} \right], \quad (5.14)$$

where the integration constant is chosen such that boundary is at  $r_\star = 0$ . We follow [7] to define the size of the gap in AC conductivity  $\omega_g$  by

$$\omega_g = \sqrt{V_{\max}}. \quad (5.15)$$

Then, we can construct an analytic expression of  $\omega_g$ . First introduce  $z_0$  at which  $V$  is maximum:

$$\left. \frac{dV}{dz} \right|_{z=z_0} = \left. \frac{d}{dz} (1-z^3)z^{2\Delta-2} F(z)^2 \right|_{z=z_0} = 0. \quad (5.16)$$

Then it can be numerically calculated as a function of  $\Delta$  and  $b$ , and the result can be fit by following expressions.

$$z_0 \approx 0.41249 \sum_{k=1}^{\infty} \frac{\sin(\pi(\Delta-1)(2k-1))}{k^{2.6376}}, \quad \text{for } 1 \leq \Delta < 2, \quad (5.17)$$

$$z_0 \approx \left( \frac{0.1}{\Delta - 1.83} + 0.7 \right) \frac{1}{b}, \quad \text{for } 2 < \Delta \leq 3. \quad (5.18)$$

Notice that from the first expression, we can see that there is no  $b$  dependence. This result is plotted in the Figure 8(a). Notice that the numerical data is fit very well by our formula. Using these data,  $\omega_g$  is given by

$$\omega_g = \sqrt{V_{\max}} = \frac{g \langle \mathcal{O}_\Delta \rangle}{r_+^{\Delta-1}} \sqrt{1 - z_0^3 z_0^{\Delta-1} F(z_0)} \approx \frac{g \langle \mathcal{O}_\Delta \rangle}{r_+^{\Delta-1}} z_0^{\Delta-1} F(z_0). \quad (5.19)$$

The expression for  $F(z_0)$  is cumbersome and it is given in the appendix A.4. The solution of Eq.(5.19) according to the regimes of  $\Delta$  is given in Table. 2 earlier in the introduction and summary section. For derivation of these results, see the appendix A.4.

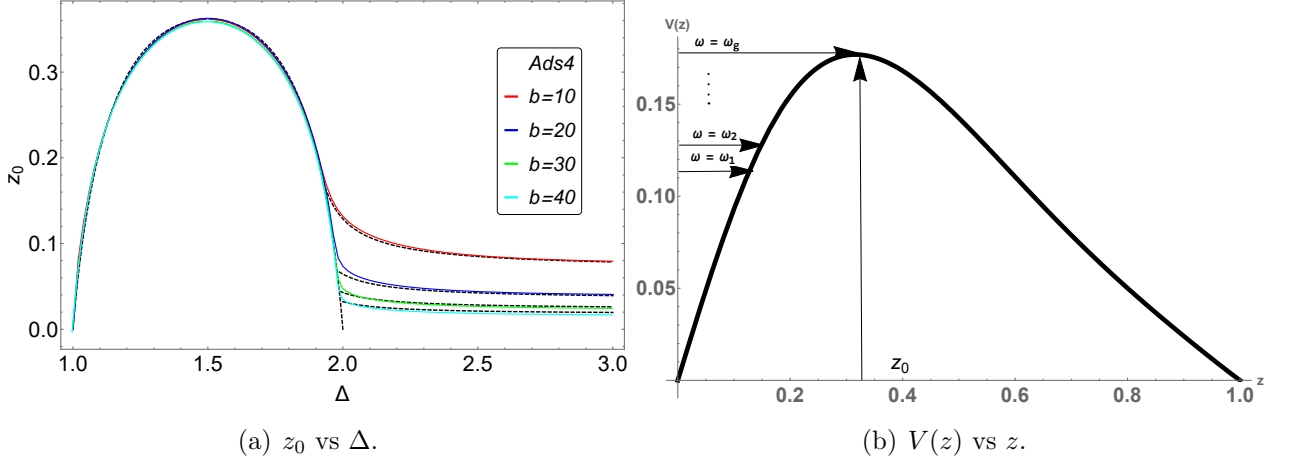


**Figure 8:** (a)  $z_0$  for various  $b$ 's. Solid colored curves are numerical expression Eq.(5.16) and dashed curves are analytic expression Eqs.(5.17, 5.18). The local maximum  $z_0 \approx 0.362$  is at  $\Delta = 3/2$ . (b) a rough picture  $V(z)$  in terms of a  $z$  coordinate.  $\omega = \omega_g$  at  $z = z_0$ .  $\omega_n$  is the  $n^{\text{th}}$  pole.  $\omega_1 < \omega_2 < \dots$  are resonant frequencies, but  $\omega_g$  is the approximate value of the gap in AC conductivities.

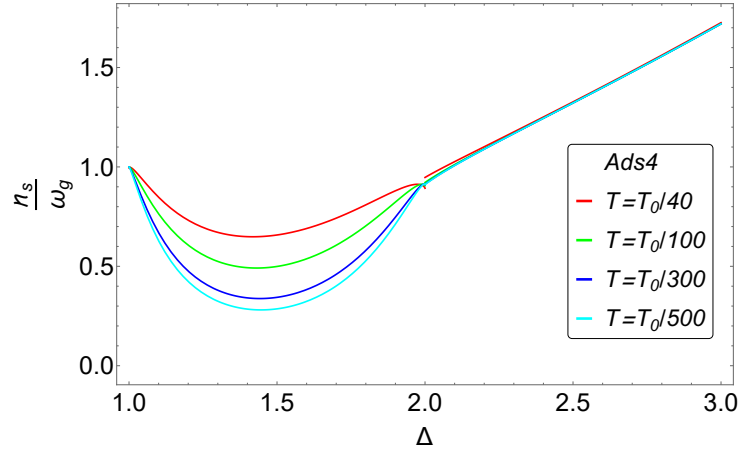


**Figure 9:**  $n_s/\omega_g$  vs  $\Delta$  for  $d = 3$ . Here,  $T_0 = (g\rho)^{\frac{1}{2}}$ . In the regime  $2 \leq \Delta \leq 3$ , it is independent of  $T$  but only  $\Delta$  dependence.

Using the result of the Cooper pair density  $n_s$  given in Eq.(1.1) and the expression of  $\omega_g$ , we can calculate the ratio  $n_s/\omega_g$ . FIG. 9 is the plot of this result. Interestingly, in the regime  $2 \leq \Delta \leq 3$ , we have linearity between  $n_s$  and  $\omega_g$ .

$$\frac{n_s}{\omega_g} \approx 0.8\Delta - 0.7,$$

Notice that in this regime of  $\Delta$ , there is no  $b$  dependence in the ratio due to the cancellation of  $b$ -dependent pieces of  $n_s$  and  $\omega_g$ .

### 5.3 The Resonant Frequencies

There is a maximum of  $z_0$  at  $\Delta = 3/2$  and the resonance, by which  $\sigma(\omega)$  diverges, occurs only in the vicinity of  $\Delta = 3/2$ . This can be understood using standard WKB matching formula. The resonance occurs when there exists  $\omega$  satisfying [14]

$$\int_{r_{*0}}^0 \sqrt{\omega^2 - V(r_*)} dr_* + \frac{\pi}{4} = n\pi,$$

for an integer  $n$  and  $r_{*0} < 0$  is the position at which  $V$  has the maximum:  $\frac{dV}{dr_*}(r_{*0}) = 0$ . The above equation can be converted to  $z$  coordinate to give the following expression:

$$\frac{1}{r_+} \int_0^{z_0} \frac{\sqrt{\omega^2 - V(z)}}{1 - z^3} dz = \left(n - \frac{1}{4}\right) \pi.$$

At  $\Delta = 3/2$ , we have

$$\int_{1/b}^{z_0} \sqrt{\left(\frac{\omega}{T_c}\right)^2 - \left(\frac{2\pi T}{3 T_c}\right)^2 b^3 z \left(\frac{4 - 3 \ln z}{2 + \ln b}\right)^2} dz = \frac{4\pi^2}{3} \left(n - \frac{1}{4}\right) \frac{T}{T_c}, \quad (5.20)$$

where  $z_0 = 0.362$  from Eq.(5.17), and

$$b = 1.23 \left(1 + 0.45 \ln \left(\frac{T_c}{T}\right)\right)^{1/4} \frac{T_c}{T},$$

$$\frac{\omega_g}{T_c} = \frac{7}{10} \frac{X^{3/2} \left(\frac{T_c}{T}\right)^{1/2}}{\ln \left(X \frac{T_c}{T}\right)}, \quad \text{with } X = \frac{g^{1/\Delta} \langle \mathcal{O}_\Delta \rangle^{1/\Delta}}{T_c}.$$

Resonant  $\omega_i$ 's exist only when  $z_0$  is large enough. We can see that  $z_0$  is maximum at  $\Delta = 3/2$  from the Fig 8(b). It turns out that only near the  $\Delta = 3/2$  because for other values which is much bigger or smaller than  $z_0$ , the barrier is too thick for the resonance to happen. For  $\frac{T}{T_c} = 0.1$ , we have  $\frac{\omega_1}{T_c} = 10.44$  which is in good agreement with the  $\omega_1/T_c = 10.4$  [7] if we set  $g = 1$ . In general, as  $T/T_c$  decreases, the number of poles increases. These results are summarized in the Table 3. For derivation of these results, see the appendix A.4.

Poles of $\sigma(\omega)$	$\frac{\omega_1}{T_c}$	$\frac{\omega_2}{T_c}$	$\frac{\omega_3}{T_c}$	$\frac{\omega_4}{T_c}$	$\frac{\omega_5}{T_c}$
$\frac{T}{T_c} = 0.1$ with $\omega_g/T_c = 10.9$	10.44				
$\frac{T}{T_c} = 0.05$ with $\omega_g/T_c = 13.4$	11.85	13.11			
$\frac{T}{T_c} = 0.04$ with $\omega_g/T_c = 14.62$	12.19	13.65	14.4		
$\frac{T}{T_c} = 0.03$ with $\omega_g/T_c = 16.34$	12.6	14.26	15.21	15.84	16.25

**Table 3:**  $\frac{\omega_n}{T_c}$  and  $\frac{T}{T_c}$  at lower  $T$ 's. where  $n = 1, 2, 3, \dots$ . A position of the pole is obtained from Eq.(5.20) with given  $\frac{T}{T_c}$  by applying Mathematica program.

## 6 Discussion

In this paper, we have shown that in holographic superconductivities,  $T_c$  has power law dependence on the coupling  $g$  so that  $T_c \sim (\rho g)^{1/2}$  unlike the BCS theory where the  $T_c$  is exponentially suppressed. We also calculated the physical observables  $T_c, \langle \mathcal{O}_\Delta \rangle, \sigma(\omega), \omega_g, \omega_i, n_s,$  as functions of  $\mathcal{O}_\Delta, T, \rho$ . Our results well agree with the numerical results of ref. [7] while we disagree with the results of [8]. Initially, we tried to follow the ref. [8]. But we had to departed from there later for many reasons. As the consequence our results are quite different from that of ref. [8]. Here we describe the main differences so that the readers understand the source of the differences in the results.

1. We use matrix algorithm by applying Pincherle's Theorem to obtain the smallest value  $\lambda_{g,3}$ . On the other hand, The authors of ref. [8] obtained the minimum value of  $\lambda_{g,3}$ 's by using variational method (see Eq.(A.28)) and they used the trial function  $F(z) = 1 - \alpha z^2$ .  $F(z)$  does not converge on the boundary of the disc of convergence at  $z = 1$  in general. However, Pincherle's Theorem tells us that  $F(z)$  converges at  $z = 1$  for some quantized value of  $\lambda_{g,3}$ . As a consequence, our methodology works straightforwardly without ambiguity caused by the divergences and effective to get an eigenvalue when a power series is made up of three or more term recurrence relation.
2. The authors of ref. [8] applied perturbation theory to obtain the condensate near  $T_c$ . It leads to the integral such as  $\mathcal{C}_3 = \int_0^1 dz \frac{z^{2(\Delta-1)} F^2(z)}{z^2+z+1}$ . Instead, we first obtain the analytic solution given by  $F(z) = (z^2 + z + 1)^{-\frac{\lambda_{g,3}}{\sqrt{3}}} \sum_{n=0}^5 d_n z^n$  (see Eq.(A.33)). Then we used it to evaluate Eq.(A.32). The result gives dramatic differences: For  $\Delta = 3$  in  $d = 3$ , we have a finite result for  $\mathcal{C}_3$ , while they claimed they got  $\mathcal{C}_3 = 0$ . As a consequence,  $g^{\frac{1}{\Delta}} \frac{\langle \mathcal{O}_\Delta \rangle^{\frac{1}{\Delta}}}{T_c}$  is finite at  $\Delta = 3$  in our result, while they have divergent result.
3. Our the boundary condition of  $F(z)$  and  $\Phi(z)$  in  $\text{AdS}_4$  is given in the following table.

Over all the regime we consider, i.e, $\frac{1}{2} < \Delta < 3$
(i) $F(0) = 1$ (nomalization of $\langle \mathcal{O} \rangle_\Delta$ $F'(0) = 0, \Phi'(0) = -\rho/r_h$
(ii) $\Phi(1) = 0, 3F'(1) + \Delta^2 F(1) = 0$

**Table 4:** Boundary condition of  $F(z)$  and  $\Phi(z)$  at the origin and the unity

On the other hand, the authors of ref. [8] used different boundary condition and different trial wave function according the regimes:  $\frac{1}{2} < \Delta < \frac{3}{2}$  and  $\frac{3}{2} < \Delta < 3$ . To compute Eq.(A.45a) and Eq.(A.45b), they applied  $K_\nu(z) \sim \frac{\Gamma(\nu)}{2} \left(\frac{2}{z}\right)^\nu$  as  $z \rightarrow 0$  into them. Because modified Bessel function  $K$  is exponentially suppressed in large

$z$ . So they thought the dominant contribution comes from near  $z = 0$  region. Unfortunately, we cannot use near zero expression of  $K_\nu$  inside the non-local double integral. In fact, using  $K_\nu(z) \sim \frac{1}{z^\nu}$  in Eq.(A.45a) gives completely different result from using the full expression of  $K_\nu(z) \sim \frac{e^{-z}}{\sqrt{z}}$ , which we did here.

Unlike in the case of  $\frac{1}{2} < \Delta < \frac{3}{2}$ , they used variational method without condition (iii) to compute  $\mathcal{A}^2$  in Eq.(A.44) in the regime  $\frac{3}{2} < \Delta < 3$ . They used different boundary condition at different region of  $\Delta$ . We believe that this is not necessary.

## Acknowledgments

We thank Ki-Seok Kim for the useful discussion. This work is supported by Mid-career Researcher Program through the National Research Foundation of Korea grant No. NRF-2021R1A2B5B0200260. We also thank the APCTP for the hospitality during the focus program, “Quantum Matter and Entanglement with Holography”, where part of this work was discussed.

## Appendices

### A Holographic superconductors with AdS<sub>4</sub>

The theory of holographic superconductors are much studied. Some of the relevant papers for the analytical techniques can be found, for example, in refs. [15–48].

#### A.1 Near the critical temperature:

##### A.1.1 Computation of $T_c$ by applying matrix algorithm and Pincherle’s Theorem

At the critical temperature  $T_c$ ,  $\Psi = 0$ , so Eq.(2.3) tells us  $\Phi'' = 0$ . Then, we can set

$$\Phi(z) = \lambda_3 r_c (1 - z) \quad \text{where } \lambda_3 = \frac{\rho}{r_c^2} \quad (\text{A.1})$$

here,  $r_c$  is the radius of the horizon at  $T = T_c$ . As  $T \rightarrow T_c$ , the field equation  $\Psi$  approaches to

$$-\frac{d^2\Psi}{dz^2} + \frac{2+z^3}{z(1-z^3)}\frac{d\Psi}{dz} + \frac{m^2}{z^2(1-z^3)}\Psi = \frac{\lambda_{g,3}^2}{(z^2+z+1)^2}\Psi \quad (\text{A.2})$$

where  $\lambda_{g,3} = g\lambda_3$ . Factoring out the behavior near the boundary  $z = 0$  and the horizon, we define

$$\Psi(z) = \frac{\langle \mathcal{O}_\Delta \rangle}{\sqrt{2}r_h^\Delta} z^\Delta F(z) \quad \text{where } F(z) = (z^2+z+1)^{-\lambda_{g,3}/\sqrt{3}} y(z) \quad (\text{A.3})$$

Then,  $F$  is normalized as  $F(0) = 1$  and we obtain

$$\begin{aligned} \frac{d^2 y}{dz^2} + \frac{(1 - \frac{4}{\sqrt{3}}\lambda_{g,3} + 2\Delta)z^3 + \frac{2\lambda_{g,3}}{\sqrt{3}}z^2 + \frac{2\lambda_{g,3}}{\sqrt{3}}z + 2(1 - \Delta)}{z(z^3 - 1)} \frac{dy}{dz} \\ + \frac{(3\Delta^2 - 4\sqrt{3}\Delta\lambda_{g,3} + 4\lambda_{g,3}^2)z^2 - (4\lambda_{g,3}^2 - 2\sqrt{3}\Delta\lambda_{g,3} - \sqrt{3}\lambda_{g,3})z - 2\sqrt{3}(1 - \Delta)\lambda_{g,3}}{3z(z^3 - 1)} y = 0. \end{aligned} \quad (\text{A.4})$$

Notice that this equation has five regular singular points at  $z = 0, 1, \frac{-1 \pm \sqrt{3}i}{2}, \infty$ . Substituting  $y(z) = \sum_{n=0}^{\infty} d_n z^n$  into (A.4), we obtain the following four term recurrence relation:

$$\alpha_n d_{n+1} + \beta_n d_n + \gamma_n d_{n-1} + \delta_n d_{n-2} = 0 \quad \text{for } n \geq 2, \quad (\text{A.5})$$

with

$$\begin{cases} \alpha_n = -3(n+1)(n+2\Delta-2) \\ \beta_n = 2\sqrt{3}\lambda_{g,3}(n+\Delta-1) \\ \gamma_n = \sqrt{3}(2n+2\Delta-3)\lambda_{g,3} - 4\lambda_{g,3}^2 \\ \delta_n = 3(n - \frac{2}{\sqrt{3}}\lambda_{g,3} + \Delta - 2)^2 \end{cases} \quad (\text{A.6})$$

The first four  $d_n$ 's are given by  $\alpha_0 d_1 + \beta_0 d_0 = 0$ ,  $\alpha_1 d_2 + \beta_1 d_1 + \gamma_1 d_0 = 0$ ,  $d_{-1} = 0$  and  $d_{-2} = 0$ . Eq.(A.3), Eq.(A.5) and Eq.(A.6) give us the following boundary condition

$$F'(0) = 0. \quad (\text{A.7})$$

Since the 4 term relation can be reduced to the 3 term relation, we first review for a minimal solution of the three term recurrence relation

$$\alpha_n d_{n+1} + \beta_n d_n + \gamma_n d_{n-1} = 0 \quad \text{for } n \geq 1, \quad (\text{A.8})$$

with  $\alpha_0 d_1 + \beta_0 d_0 = 0$  and  $d_{-1} = 0$ . Eq.(A.8) has two linearly independent solutions  $X(n)$ ,  $Y(n)$ . We recall that  $\{X(n)\}$  is a minimal solution of Eq.(A.8) if not all  $X(n) = 0$  and if there exists another solution  $Y(n)$  such that  $\lim_{n \rightarrow \infty} X(n)/Y(n) = 0$ . Now  $(d_n)_{n \in \mathbb{N}}$  is the minimal solution if  $\alpha_0 \neq 0$  and

$$\beta_0 + \frac{-\alpha_0 \gamma_1}{\beta_1 - \frac{\alpha_1 \gamma_2}{\beta_2 - \frac{\alpha_2 \gamma_3}{\beta_3 - \dots}}} = 0. \quad (\text{A.9})$$

One should remember that  $\alpha_n, \beta_n, \gamma_n$ 's are functions of  $\lambda$  so that above equation should be read as equation for  $\lambda$ .

As we mentioned above, we can transform the four term recurrence relations into three-term recurrence relations by the Gaussian elimination steps. More explicitly, the transformed recurrence relation is

$$\alpha'_n d_{n+1} + \beta'_n d_n + \gamma'_n d_{n-1} = 0 \quad \text{for } n \geq 1, \quad (\text{A.10})$$

where

$$\alpha'_n = \alpha_n, \quad \beta'_n = \beta_n, \quad \gamma'_n = \gamma_n \quad \text{for } n = 0, 1$$

and

$$\begin{cases} \delta'_n = 0 \\ \alpha'_n = \alpha_n \\ \beta'_n = \beta_n - \frac{\alpha'_{n-1} \delta_n}{\gamma'_{n-1}} \\ \gamma'_n = \gamma_n - \frac{\beta'_{n-1} \delta_n}{\gamma'_{n-1}} \end{cases} \quad \text{for } n \geq 2 \quad (\text{A.11})$$



So for a four-term recurrence relation in Eq.(A.5), the radius of convergence is 1 for all three cases. Since the solutions should converge at the horizon,  $y(z)$  should be convergent at  $|z| \leq 1$ . According to Pincherle's Theorem [52], we have a convergent solution of  $y(z)$  at  $|z| = 1$  if only if the four term recurrence relation Eq.(A.5) has a minimal solution. Since we have three different roots  $\rho_i$ 's, so Eq.(A.15) has three linearly independent solutions  $d_1(n), d_2(n), d_3(n)$ . One can show that [52] for the large  $n$ ,

$$d_i(n) \sim \rho_i^n n^{\alpha_i} \sum_{r=0}^{\infty} \frac{\tau_i(r)}{n^r}, \quad i = 1, 2, 3 \quad (\text{A.20})$$

with

$$\alpha_i = \frac{a_1 \rho_i^2 + b_1 \rho_i + c_1}{a_0 \rho_i^2 + 2b_0 \rho_i + c_0}, \quad i = 1, 2, 3 \quad (\text{A.21})$$

and  $\tau_i(0) = 1$ . In particular, we obtain

$$\tau_i(1) = \frac{(-a_0 \rho_i^2 + 3c_0)\alpha_i^2 + (a_0 \rho_i^2 - 2b_1 \rho_i - 3c_0 - 4c_1)\alpha_i + 2(a_2 \rho_i^2 + b_2 \rho_i + c_2)}{2(a_0 \rho_i^2 + 2b_0 \rho_i + 3c_0)\alpha_i - 2((a_0 + a_1)\rho_i^2 + (b_1 + 2b_0)\rho_i + c_1 + 3c_0)}, \quad i = 1, 2, 3 \quad (\text{A.22})$$

Substituting Eq.(A.19) and Eq.(A.17) into Eq.(A.20)–Eq.(A.22), we obtain

$$\begin{cases} d_1(n) \sim n^{-1} \left( 1 + \frac{-3\Delta^2 + (3\sqrt{3} - 4\lambda_{g,3})\lambda_{g,3}}{9n} \right) \\ d_2(n) \sim \left( \frac{-1 + \sqrt{3}i}{2} \right)^n n^{-1 - \frac{2\lambda_{g,3}}{\sqrt{3}}} \left( 1 + \frac{\varpi - \chi i}{n} \right) \\ d_3(n) \sim \left( \frac{-1 - \sqrt{3}i}{2} \right)^n n^{-1 - \frac{2\lambda_{g,3}}{\sqrt{3}}} \left( 1 + \frac{\varpi + \chi i}{n} \right) \end{cases} \quad (\text{A.23})$$

with

$$\begin{cases} \varpi = \frac{-6\Delta^2 - 12\sqrt{3}\Delta\lambda_{g,3} + (15\sqrt{3} + 16\lambda_{g,3})\lambda_{g,3}}{18} \\ \chi = \frac{(3 + 4\sqrt{3})\lambda_{g,3}}{18} \end{cases} \quad (\text{A.24})$$

Since  $\lambda_{g,3} > 0$ ,

$$\lim_{n \rightarrow \infty} \frac{d_2(n)}{d_1(n)} = 0, \quad \lim_{n \rightarrow \infty} \frac{d_3(n)}{d_1(n)} = 0. \quad (\text{A.25})$$

Therefore  $d_2(n)$  and  $d_3(n)$  are minimal solutions. Also,

$$\begin{cases} \sum |d_1(n)| \sim \sum \frac{1}{n} \rightarrow \infty \\ \sum |d_2(n)| \sim \sum n^{-1 - \frac{2\lambda_{g,3}}{\sqrt{3}}} < \infty \\ \sum |d_3(n)| \sim \sum n^{-1 - \frac{2\lambda_{g,3}}{\sqrt{3}}} < \infty \end{cases} \quad (\text{A.26})$$

Therefore,  $y(z) = \sum_{n=0}^{\infty} d_n z^n$  is convergent at  $z = 1$  if only if we take  $d_2$  and  $d_3$  which are minimal solutions.

Eq.(A.13) becomes a polynomial of degree  $N$  with respect to  $\lambda_{g,3}$ . The algorithm to find  $\lambda_{g,3}$  for a given  $\Delta$  is simple:

1. Choose an  $N$ .
2. Define a function returning the determinant of system Eq.(A.13).
3. Find the roots of interest of this function.
4. Increase  $N$  until those roots become constant to within the desired precision [10].

We use Mathematica to compute the determinants to locate their roots. We are only interested in smallest positive real roots of  $\lambda_{g,3}$  because of a physical condition. For computation of roots, we choose  $N = 15$ . For the smallest value of  $\lambda_{g,3}$ , we can find an approximate fitting function that is given by

$$\lambda_{g,3} \approx 4.09 (\Delta - 1/2)^{1/3} \left( \Delta^{0.7} + \left( \frac{-0.97\Delta + 0.12}{\Delta - 0.07} \right)^5 \right) \quad (\text{A.27})$$

We calculated 101 different values of  $\lambda_{g,3}$ 's at various  $\Delta$  and the result is the red colored dots in Fig. 10(a). These data fits well by above formula. The log-log plot of Fig. 10(b) shows that the exponent of  $(\Delta - 1/2)$  is  $1/3$  with high precision.

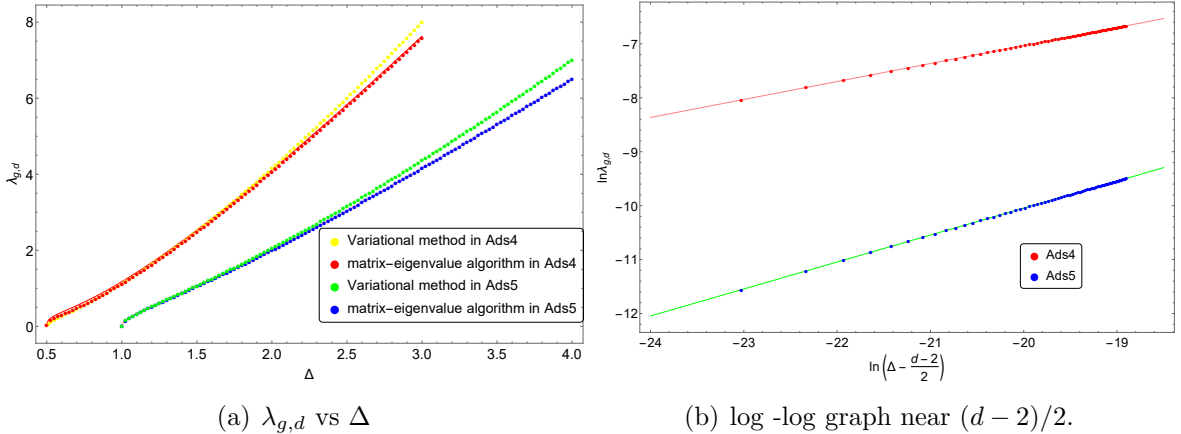


**Figure 10:** (a)  $\lambda_{g,d}$  vs  $\Delta$ : red colored dots for  $\lambda_{g,3}$  and blue dots for  $\lambda_{g,4}$  are fit well with eq.(3.5) represented by the real lines with the same colors. The results of variational method in ref. [8] is denoted by yellow and green dots for AdS<sub>4</sub> and AdS<sub>5</sub> respectively.

(b) The slope of red dotted line for  $\ln \lambda_{g,3}$  is  $1/3$ , and the slope of blue dots for  $\ln \lambda_{g,4}$  is  $1/2$ .

The authors of ref.[8] got  $\lambda_{g,3}$ 's by using variational method using the fact that the eigenvalue  $\lambda_{g,3}$  minimizes the expression

$$\lambda_{g,3}^2 = \frac{\int_0^1 dz z^{2\Delta-2} \left( (1-z^3) [F'(z)]^2 + \Delta^2 z [F(z)]^2 \right)}{\int_0^1 dz z^{2\Delta-2} \frac{1-z}{1+z+z^2} [F(z)]^2}. \quad (\text{A.28})$$

for  $\Delta > 1/2$ . The integral does not converge at  $\Delta = 1/2$  because of  $\ln(z)$ . The trial function used is  $F(z) = 1 - \alpha z^2$  where  $\alpha$  is the variational parameter. Their result is given by the blue colored dots in Fig. 10(a).

Notice that the minimum  $\lambda_{g,3}$  is zero at  $\Delta = 1/2$  in Eq.(A.13). However, we cannot choose  $\lambda_{g,3} = 0$  as our analytic solution. Because, if so,  $y(z)$  is divergent at  $z = 1$  as we can see from Eq.(A.26). It means that  $\lim_{\Delta \rightarrow 1/2} \lambda_{g,3} = 0$  but  $y(z)$  is not defined at  $\Delta = 1/2$ . Also, we cannot obtain the smallest root of  $\lambda_{g,3}$  for  $\Delta = 1$ , and we have only a trivial solution of  $\lambda_{g,3}$  as we see Eq.(A.13) because  $\alpha_0 = \beta_0 = 0$ . Instead of using Eq.(A.13), we can have a proper root by applying Eq.(A.14).

The critical temperature is given by  $T_c = \frac{3}{4\pi} r_c = \frac{3}{4\pi} \sqrt{\frac{\rho}{\lambda_3}}$ , which can be calculated by Eq.(A.27) and the Fig. 11 demonstrate the result. Notice that  $T_c$  is divergent at  $\Delta = 1/2$  and it is a monotonically decreasing function of  $\Delta$ .

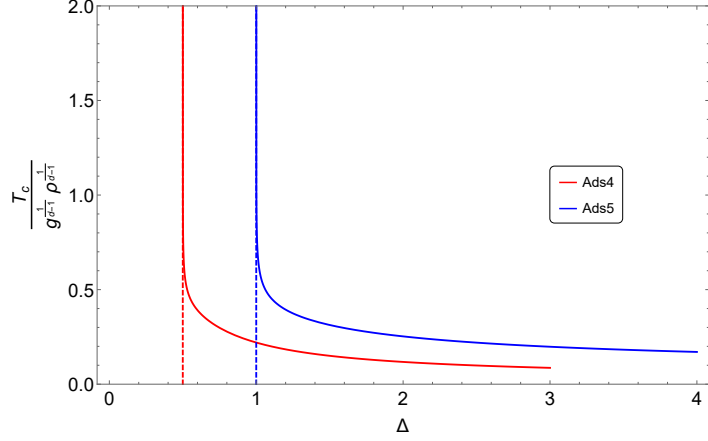


**Figure 11:**  $\frac{T_c}{\rho^{\frac{1}{d-1}} g^{\frac{1}{d-1}}}$  as functions of  $\Delta$ .

### A.1.2 An analytic solution of $g \frac{\langle \mathcal{O}_\Delta \rangle}{T_c^\Delta}$

Substituting Eq.(A.3) into Eq.(2.3), the field equation  $\Phi$  becomes

$$\frac{d^2 \Phi}{dz^2} = \frac{g^2 \langle \mathcal{O}_\Delta \rangle^2}{r_h^{2\Delta}} \frac{z^{2(\Delta-1)} F^2(z)}{1-z^3} \Phi, \quad (\text{A.29})$$

where  $g \langle \mathcal{O}_\Delta \rangle^2 / r_h^{2\Delta}$  is small because  $T \approx T_c$ . The above equation have the expansion around Eq.(A.1) with small correction [8]:

$$\frac{\Phi}{r_h} = \lambda_3 (1-z) + \frac{g^2 \langle \mathcal{O}_\Delta \rangle^2}{r_h^{2\Delta}} \chi_1(z) \quad (\text{A.30})$$

We have  $\chi_1(1) = \chi_1'(1) = 0$  due to the boundary condition  $\Phi(1) = 0$ . Taking the derivative of Eq.(A.30) twice with respect to  $z$  and using the result in Eq.(A.29),

$$\chi_1'' = \frac{z^{2(\Delta-1)} F^2(z)}{1-z^3} \left\{ \lambda_3 (1-z) + \frac{g^2 \langle \mathcal{O}_\Delta \rangle^2}{r_h^{2\Delta}} \chi_1 \right\} \approx \frac{\lambda_3 z^{2(\Delta-1)} F^2(z)}{z^2 + z + 1}. \quad (\text{A.31})$$

Integrating Eq.(A.31) gives us

$$\chi_1'(0) = -\lambda_3 \mathcal{C}_3 \quad \text{for } \mathcal{C}_3 = \int_0^1 dz \frac{z^{2(\Delta-1)} F^2(z)}{z^2 + z + 1}. \quad (\text{A.32})$$

Eq.(A.3) with Eq.(A.6) shows

$$F(z) = (z^2 + z + 1)^{-\lambda_{g,3}/\sqrt{3}} y(z) \approx (z^2 + z + 1)^{-\frac{\lambda_{g,3}}{\sqrt{3}}} \sum_{n=0}^5 d_n z^n. \quad (\text{A.33})$$

Here, we ignore  $d_n z^n$  terms if  $n \geq 6$  because  $0 < |d_n| \ll 1$  numerically and  $y(z)$  converges for  $0 < z \leq 1$ . Putting Eq.(A.33) into Eq.(A.32), we have

$$\begin{aligned} \mathcal{C}_3 = & \mathcal{J}_1 F_1 \left( 2\Delta - 1; \widetilde{\lambda}_{g,3}, \widetilde{\lambda}_{g,3}; 2\Delta; (-1)^{2/3}, -\sqrt[3]{-1} \right) + \mathcal{J}_2 F_1 \left( 2\Delta; \widetilde{\lambda}_{g,3}, \widetilde{\lambda}_{g,3}; 2\Delta + 1; (-1)^{2/3}, -\sqrt[3]{-1} \right) \\ & + \mathcal{J}_3 F_1 \left( 2\Delta + 1; \widetilde{\lambda}_{g,3}, \widetilde{\lambda}_{g,3}; 2(\Delta + 1); (-1)^{2/3}, -\sqrt[3]{-1} \right) + \mathcal{J}_4 F_1 \left( 2\Delta + 1; \widetilde{\lambda}_{g,3} + 1, \widetilde{\lambda}_{g,3} + 1; 2(\Delta + 1); (-1)^{2/3}, -\sqrt[3]{-1} \right) \\ & + \mathcal{J}_5 F_1 \left( 2(\Delta + 1); \widetilde{\lambda}_{g,3}, \widetilde{\lambda}_{g,3}; 2\Delta + 3; (-1)^{2/3}, -\sqrt[3]{-1} \right) + \mathcal{J}_6 F_1 \left( 2(\Delta + 1); \widetilde{\lambda}_{g,3} + 1, \widetilde{\lambda}_{g,3} + 1; 2\Delta + 3; (-1)^{2/3}, -\sqrt[3]{-1} \right) \\ & + \mathcal{J}_7 F_1 \left( 2\Delta + 3; \widetilde{\lambda}_{g,3}, \widetilde{\lambda}_{g,3}; 2(\Delta + 2); (-1)^{2/3}, -\sqrt[3]{-1} \right) + \mathcal{J}_8 F_1 \left( 2(\Delta + 2); \widetilde{\lambda}_{g,3}, \widetilde{\lambda}_{g,3}; 2\Delta + 5; (-1)^{2/3}, -\sqrt[3]{-1} \right) \\ & + \mathcal{J}_9 F_1 \left( 2\Delta + 5; \widetilde{\lambda}_{g,3}, \widetilde{\lambda}_{g,3}; 2(\Delta + 3); (-1)^{2/3}, -\sqrt[3]{-1} \right) + \mathcal{J}_{10} F_1 \left( 2(\Delta + 3); \widetilde{\lambda}_{g,3}, \widetilde{\lambda}_{g,3}; 2\Delta + 7; (-1)^{2/3}, -\sqrt[3]{-1} \right) \\ & + \mathcal{J}_{11} F_1 \left( 2\Delta + 7; \widetilde{\lambda}_{g,3}, \widetilde{\lambda}_{g,3}; 2(\Delta + 4); (-1)^{2/3}, -\sqrt[3]{-1} \right), \end{aligned} \quad (\text{A.34})$$

with

$$\left\{ \begin{aligned} \mathcal{J}_1 &= \frac{1}{2\Delta-1} \\ \mathcal{J}_2 &= \frac{2d_1-1}{2\Delta} \\ \mathcal{J}_3 &= \frac{2(d_1(d_3-d_4)+d_4-d_5)+(d_2-d_4+d_5)(d_2-2d_3+d_4+d_5)}{2\Delta+1} \\ \mathcal{J}_4 &= \frac{(d_1-d_2+d_4-d_5)(d_1+d_2-2d_3+d_4+d_5-2)}{2\Delta+1} \\ \mathcal{J}_5 &= \frac{2(d_1(d_4-d_5)+d_5)-(d_3-d_4)(-2d_2+d_3+d_4-2d_5)}{2(\Delta+1)} \\ \mathcal{J}_6 &= \frac{(2d_1-d_2-d_3+2d_4-d_5-1)(d_2-d_3+d_5-1)}{\Delta+1} \\ \mathcal{J}_7 &= \frac{(d_3-d_5)(d_3-2d_4+d_5)+2(d_2(d_4-d_5)+d_1d_5)}{2\Delta+3} \\ \mathcal{J}_8 &= \frac{-d_4^2+2d_3(d_4-d_5)+d_5(2d_2+d_5)}{2(\Delta+2)} \\ \mathcal{J}_9 &= \frac{d_4^2-2d_5d_4+2d_3d_5}{2\Delta+5} \\ \mathcal{J}_{10} &= \frac{(2d_4-d_5)d_5}{2(\Delta+3)} \\ \mathcal{J}_{11} &= \frac{d_5^2}{2\Delta+7} \\ \widetilde{\lambda}_g &= \frac{2\lambda_{g,3}}{\sqrt{3}} \end{aligned} \right.$$

at  $\Delta > 1/2$ . Notice that the Appell hypergeometric function  $F_1$  of two variables has series expansion

$$F_1(a; b_1, b_2; c; x, y) = \sum_{n=0}^{\infty} \sum_{m=0}^{\infty} (a)_{n+m} (b_1)_m (b_2)_n / ((c)_{n+m} n! m!) x^m y^n.$$

We can calculate the numerical value of  $\mathcal{C}_3$  by putting Eq.(A.27) and Eq.(A.6) into Eq.(A.34). We calculated 102 different values of  $\mathcal{C}_3$ 's at various  $\Delta$ , which is drawn as dots

in Fig. 12. Then we tried to find an approximate fitting function. The result is given as follows,

$$\mathcal{C}_3 \approx \frac{(\Delta^5 - 5.75\Delta^4 + 13.38\Delta^3 - 14.46\Delta^2 + 8.45\Delta - 1.35)^{-1}}{\pi(\Delta - \frac{1}{2})} \quad (\text{A.35})$$

The Fig. 12 shows how the data fits by above formula. It is important to note that the

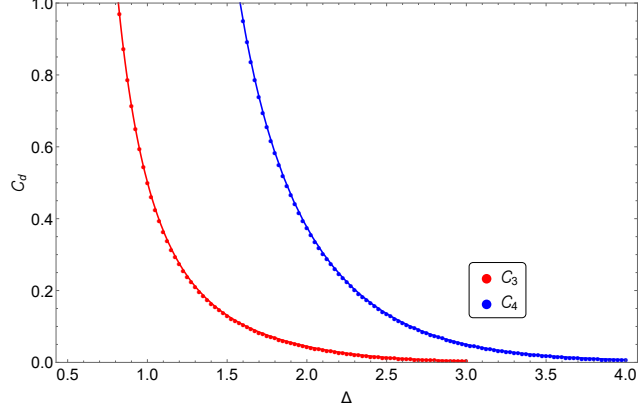


**Figure 12:** (a)  $\mathcal{C}_3$  data by eq.(A.34) with eq.(A.27), as functions of  $\Delta$ . (b)  $\mathcal{C}_4$  data by eq.(B.26) with eq.(B.19), as functions of  $\Delta$ ,

integral for  $\mathcal{C}_3$  in Eq.(A.32) diverges at  $\Delta = 1/2$ . From the Eq.(A.30) and Eq.(2.4), we have

$$\frac{\rho}{r_h^2} = \lambda_3 \left( 1 + \frac{\mathcal{C}_3 g^2 \langle \mathcal{O}_\Delta \rangle^2}{r_h^{2\Delta}} \right) \quad (\text{A.36})$$

Putting  $T = \frac{3}{4\pi} r_h$  with  $\lambda_3 = \frac{\rho}{r_h^2}$  into Eq.(A.36), we obtain the condensate near  $T_c$ :

$$g \frac{\langle \mathcal{O}_\Delta \rangle}{T_c^\Delta} \approx \mathcal{M}_3 \sqrt{1 - \frac{T}{T_c}} \quad \text{for } \mathcal{M}_3 = \left( \frac{4\pi}{3} \right)^\Delta \sqrt{\frac{2}{\mathcal{C}_3}} \quad (\text{A.37})$$

In ref. [8] it was argued that  $\lim_{\Delta \rightarrow d} \mathcal{C}_d = 0$ , which would lead to the divergence of the condensation in eq. (4.1). However, our result shows that  $\lim_{\Delta \rightarrow d} \mathcal{C}_d = \text{finite}$  so that eq. (4.1) is finite, which can be confirmed in the FIG. 13. The condensate is an increasing function of the  $\Delta$  but it decreases with increasing  $T$ .

## A.2 Condensate near the zero temperature

In general, Eq.(2.3) shows us that  $F(z)$  in Eq. (A.3) does not converge at  $z = 1$ . But the previous section A.1.1 says that it is converged at the horizon with specific value of  $\langle \mathcal{O}_\Delta \rangle$ . Its means whether we can find eigenvalue of it at  $z = 1$  or not simply, satisfied for  $F(1) < \infty$ . Unlike  $T \approx T_c$  case, it is really hard to find the eigenvalue  $\langle \mathcal{O}_\Delta \rangle$  at  $T \approx 0$ . Because Eq.(2.3) are nonlinear coupled equations:  $\Phi(z)$  cannot be described in a linear equation any longer unlike  $T \approx T_c$  case. Instead, we use the perturbation theory for the eigenvalue at  $T \approx 0$ .

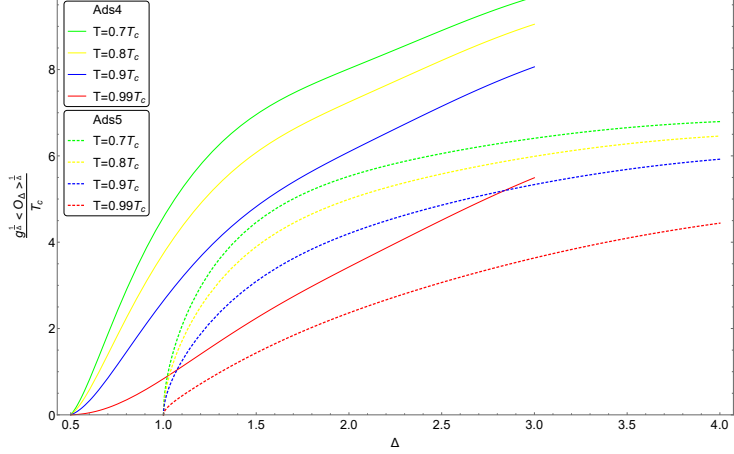


**Figure 13:**  $g^{\frac{1}{\Delta}} \langle \mathcal{O}_\Delta \rangle^{\frac{1}{\Delta}} / T_c$  vs  $\Delta$  for a few  $T$ 's near  $T_c$ . Solid curves are for AdS<sub>4</sub> and dotted ones are for AdS<sub>5</sub>.

### A.2.1 Analytic calculation of $g^{\frac{1}{\Delta}} \langle \mathcal{O}_\Delta \rangle^{\frac{1}{\Delta}} / T_c$ at $1/2 < \Delta < 3$

The Hawking temperature shows  $r_h \rightarrow 0$  as  $T \rightarrow 0$ . We can say  $z = r_h/r \rightarrow 0$  at  $r \gg r_h$  and the dominant contribution comes from the neighborhood of the boundary  $z = 0$ . So near the  $T = 0$  we can simplify two coupled equations Eq.(2.3) and Eq.(2.3) with Eq.(A.3) by letting  $z \rightarrow 0$ :

$$\frac{d^2 F}{dz^2} + \frac{2(\Delta - 1)}{z} \frac{dF}{dz} + \frac{g^2 \Phi^2}{r_h^2} F = 0 \quad (\text{A.38a})$$

$$\frac{d^2 \Phi}{dz^2} - \frac{g^2 \langle \mathcal{O}_\Delta \rangle^2}{r_h^{2\Delta}} z^{2(\Delta-1)} F^2 \Phi = 0. \quad (\text{A.38b})$$

We use a boundary condition at the horizon, and Eq.(2.3) with Eq.(A.3) is rewritten as

$$-\frac{d^2 F}{dz^2} + \left( \frac{2 + z^3}{z(1 - z^3)} - \frac{2\Delta}{z} \right) \frac{dF}{dz} + \left( \frac{\Delta^2 z}{1 - z^3} - \frac{g^2 \Phi^2}{r_h^2 (1 - z^3)^2} \right) F = 0 \quad (\text{A.39})$$

and it provides us the following boundary condition at the horizon with Eq.(2.3),  $\Phi(1) = 0$  and  $\Psi(1) < \infty$ :

$$3F'(1) + \Delta^2 F(1) = 0. \quad (\text{A.40})$$

By multiplying  $z$  to the eq. (A.39) and then taking the limit of  $z \rightarrow 0$ , we get  $F'(0) = 0$ . Note that  $F(0) = 1$  should be considered as the normalization condition of  $\langle \mathcal{O}_\Delta \rangle$  rather than as a boundary condition. Also for canonical system, we regard the  $\Phi'(0) = -\frac{\rho}{r_h}$  as BC and  $\Phi(0) = \mu$  is not a BC but a value that should be determined by  $\rho$  from the horizon regularity condition  $\Phi(1) = 0$ . In Grand canonical system  $\Phi(0) = \mu$  is the boundary condition and  $\rho$  should be determined from it by the  $\Phi(1) = 0$ . Here we consider  $\rho$  as the given parameter.

If we introduce  $b$  by for  $b^\Delta = \frac{g \langle \mathcal{O}_\Delta \rangle}{\Delta r_h^\Delta}$ , the solution to Eq.(A.38b) for  $\Phi$  with  $F \approx 1$  is

$$\Phi(z) = \mathcal{A} r_h \sqrt{bz} K_{\frac{1}{2\Delta}}(b^\Delta z^\Delta) \quad (\text{A.41})$$

At the horizon  $\Phi(1) \propto \exp(-b^\Delta) \rightarrow 0$  because  $b \rightarrow \infty$  as  $r_h \rightarrow 0$  ( $T \rightarrow 0$ ), which takes care the boundary condition  $\Phi(1) = 0$ . Substituting Eq.(A.41) into Eq.(A.38a),  $F$  becomes

$$\frac{d^2 F}{dz^2} + \frac{2(\Delta - 1)}{z} \frac{dF}{dz} + g^2 b \mathcal{A}^2 z \left( K_{\frac{1}{2\Delta}}(b^\Delta z^\Delta) \right)^2 F = 0. \quad (\text{A.42})$$

$F(z)$  can be obtained iteratively starting from  $F = 1$ . The result is

$$F(z) = 1 - g^2 b \mathcal{A}^2 \int_0^z dz \tilde{z}^{2(1-\Delta)} \int_0^{\tilde{z}} d\tilde{z} \tilde{z}^{2\Delta-1} \left( K_{\frac{1}{2\Delta}}(b^\Delta \tilde{z}^\Delta) \right)^2 \quad (\text{A.43a})$$

$$F'(z) = -g^2 b \mathcal{A}^2 z^{2(1-\Delta)} \int_0^z d\tilde{z} \tilde{z}^{2\Delta-1} \left( K_{\frac{1}{2\Delta}}(b^\Delta \tilde{z}^\Delta) \right)^2 \quad (\text{A.43b})$$

with the boundary condition  $F'(0) = 0$  and normalized  $F(0) = 1$ . Applying the boundary condition Eq.(A.40) into Eq.(A.43a) and Eq.(A.43b), we obtain

$$g^2 \mathcal{A}^2 = \frac{\Delta^2 b^2}{3F'_\Delta(b) + \Delta^2 F_\Delta(b)} \quad (\text{A.44})$$

where

$$F_\Delta(b) = \int_0^b dz z^{2-2\Delta} \int_0^z d\tilde{z} \tilde{z}^{2\Delta-1} \left( K_{\frac{1}{2\Delta}}(\tilde{z}^\Delta) \right)^2 \quad (\text{A.45a})$$

$$F'_\Delta(b) = b^{3-2\Delta} \int_0^b dz z^{2\Delta-1} \left( K_{\frac{1}{2\Delta}}(z^\Delta) \right)^2. \quad (\text{A.45b})$$

With  $x = z^\Delta$ , Eq.(A.45b) is simplified as

$$F'_\Delta(b) = \frac{b^{3-2\Delta}}{\Delta} \int_0^{b^\Delta} dx x \left( K_{\frac{1}{2\Delta}}(x) \right)^2 \approx \frac{b^{3-2\Delta}}{\Delta} \int_0^\infty dx x \left( K_{\frac{1}{2\Delta}}(x) \right)^2. \quad (\text{A.46})$$

There is the integral formula [53]:

$$\int_0^\infty dx x^{-\lambda} K_\mu(x) K_\nu(x) = \frac{2^{-2-\lambda}}{\Gamma(1-\lambda)} \Gamma\left(\frac{1-\lambda+\mu+\nu}{2}\right) \Gamma\left(\frac{1-\lambda-\mu+\nu}{2}\right) \Gamma\left(\frac{1-\lambda+\mu-\nu}{2}\right) \Gamma\left(\frac{1-\lambda-\mu-\nu}{2}\right) \quad (\text{A.47})$$

where  $Re \lambda < 1 - |Re \mu| - |Re \nu|$ . Using Eq.(A.47), Eq.(A.46) becomes

$$F'_\Delta(b) = \frac{\pi}{4\Delta^2} \csc\left(\frac{\pi}{2\Delta}\right) b^{3-2\Delta} \quad (\text{A.48})$$

Letting  $x = \tilde{z}^\Delta$ , Eq.(A.45a) is simplified as

$$F_\Delta(b) = \frac{1}{\Delta} \int_0^b dz z^{2-2\Delta} \int_0^{z^\Delta} dx x \left( K_{\frac{1}{2\Delta}}(x) \right)^2 \quad (\text{A.49})$$

We have the following integral formula:

$$\int dx x (K_\nu(x))^2 = \frac{x^2}{2} \left\{ (K_\nu(x))^2 - K_{\nu-1}(x) K_{\nu+1}(x) \right\}. \quad (\text{A.50})$$

And

$$\lim_{x \rightarrow 0} K_\nu(x) = \frac{\Gamma(\nu)}{2} \left(\frac{x}{2}\right)^{-\nu} + \frac{\Gamma(-\nu)}{2} \left(\frac{x}{2}\right)^\nu \quad (\text{A.51})$$

As we apply Eq.(A.47), Eq.(A.50) and Eq.(A.51) into Eq.(A.49), we obtain

$$\begin{aligned} F_\Delta(b) &= \frac{\pi b^{3-2\Delta}}{4\Delta^2(3-2\Delta)} \csc\left(\frac{\pi}{2\Delta}\right) - \frac{\pi \epsilon^{3-2\Delta}}{4\Delta^2(3-2\Delta)} \csc\left(\frac{\pi}{2\Delta}\right) \\ &+ \frac{1}{2\Delta^2} \lim_{\epsilon \rightarrow 0} \int_{\epsilon^\Delta}^{b^\Delta} dx x^{\frac{3-\Delta}{2\Delta}} K_{\frac{1}{2\Delta}}(x)^2 - \frac{1}{2\Delta^2} \lim_{\epsilon \rightarrow 0} \int_{\epsilon^\Delta}^{b^\Delta} dx x^{\frac{3-\Delta}{2\Delta}} K_{\frac{1}{2\Delta}-1}(x) K_{\frac{1}{2\Delta}+1}(x) \\ &\approx \frac{\pi b^{3-2\Delta}}{4\Delta^2(3-2\Delta)} \csc\left(\frac{\pi}{2\Delta}\right) - \frac{\pi \epsilon^{3-2\Delta}}{4\Delta^2(3-2\Delta)} \csc\left(\frac{\pi}{2\Delta}\right) \\ &+ \frac{1}{2\Delta^2} \int_0^\infty dx x^{\frac{3-\Delta}{2\Delta}} K_{\frac{1}{2\Delta}}(x)^2 - \frac{1}{2\Delta^2} \lim_{\epsilon \rightarrow 0} \int_{\epsilon^\Delta}^{b^\Delta} dx x^{\frac{3-\Delta}{2\Delta}} K_{\frac{1}{2\Delta}-1}(x) K_{\frac{1}{2\Delta}+1}(x) \\ &= \frac{\pi b^{3-2\Delta}}{4\Delta^2(3-2\Delta)} \csc\left(\frac{\pi}{2\Delta}\right) - \frac{\pi \epsilon^{3-2\Delta}}{4\Delta^2(3-2\Delta)} \csc\left(\frac{\pi}{2\Delta}\right) \\ &+ \frac{\sqrt{\pi} \Gamma\left(\frac{1}{\Delta}\right) \Gamma\left(\frac{3}{2\Delta}\right) \Gamma\left(\frac{2}{\Delta}\right)}{8\Delta^2 \Gamma\left(\frac{3+2\Delta}{2\Delta}\right)} - \frac{1}{2\Delta^2} \lim_{\epsilon \rightarrow 0} \int_{\epsilon^\Delta}^{b^\Delta} dx x^{\frac{3-\Delta}{2\Delta}} K_{\frac{1}{2\Delta}-1}(x) K_{\frac{1}{2\Delta}+1}(x) \quad (\text{A.52}) \end{aligned}$$

here, we introduce small  $\epsilon$ , and take zero at the end of calculations.

There are two different formulas:

$$\begin{aligned} \int dx x^\lambda K_\nu(x) K_\mu(x) &= \pi^2 2^{-\mu-\nu-3} \csc(\pi\mu) \csc(\pi\nu) x^{\lambda-\mu-\nu+1} \left\{ 4^{\mu+\nu} \Gamma(-\mu-\nu+1) \Gamma\left(\frac{1}{2}(\lambda-\mu-\nu+1)\right) \right. \\ &\times {}_3F_4 \left[ \begin{matrix} \frac{1}{2}(-\mu-\nu+1), \frac{1}{2}(-\mu-\nu+2), \frac{1}{2}(\lambda-\mu-\nu+1) \\ 1-\mu, 1-\nu, -\mu-\nu+1, \frac{1}{2}(\lambda-\mu-\nu+3) \end{matrix}; x^2 \right] \\ &- 4^\nu x^{2\mu} \Gamma(\mu-\nu+1) \Gamma\left(\frac{1}{2}(\lambda+\mu-\nu+1)\right) {}_3F_4 \left[ \begin{matrix} \frac{1}{2}(\mu-\nu+1), \frac{1}{2}(\mu-\nu+2), \frac{1}{2}(\lambda+\mu-\nu+1) \\ \mu+1, 1-\nu, \mu-\nu+1, \frac{1}{2}(\lambda+\mu-\nu+3) \end{matrix}; x^2 \right] \\ &- 4^\mu x^{2\nu} \Gamma(-\mu+\nu+1) \Gamma\left(\frac{1}{2}(\lambda-\mu+\nu+1)\right) {}_3F_4 \left[ \begin{matrix} \frac{1}{2}(-\mu+\nu+1), \frac{1}{2}(-\mu+\nu+2), \frac{1}{2}(\lambda-\mu+\nu+1) \\ 1-\mu, \frac{1}{2}(\lambda-\mu+\nu+3), \nu+1, -\mu+\nu+1 \end{matrix}; x^2 \right] \\ &\left. + \Gamma(\mu+\nu+1) x^{2\mu+2\nu} \Gamma\left(\frac{1}{2}(\lambda+\mu+\nu+1)\right) {}_3F_4 \left[ \begin{matrix} \frac{1}{2}(\mu+\nu+1), \frac{1}{2}(\mu+\nu+2), \frac{1}{2}(\lambda+\mu+\nu+1) \\ \mu+1, \frac{1}{2}(\lambda+\mu+\nu+3), \nu+1, \mu+\nu+1 \end{matrix}; x^2 \right] \right\} \quad (\text{A.53}) \end{aligned}$$

$${}_pF_q \left[ \begin{matrix} a, a_2, \dots, a_p \\ a-1, b_2, \dots, b_q \end{matrix}; z \right] = {}_{p-1}F_{q-1} \left[ \begin{matrix} a_2, \dots, a_p \\ b_2, \dots, b_q \end{matrix}; z \right] + \frac{z a_2 \dots a_p}{(a-1) b_2 \dots b_q} {}_{p-1}F_{q-1} \left[ \begin{matrix} a_2+1, \dots, a_p+1 \\ b_2+1, \dots, b_q+1 \end{matrix}; z \right] \quad (\text{A.54})$$

And the asymptotic formula for the  ${}_2F_3$  hypergeometric function as  $|z| \rightarrow \infty$  is written by[54]:

$$\begin{aligned} {}_2F_3 \left[ \begin{matrix} a_1, a_2 \\ b_1, b_2, b_3 \end{matrix}; z \right] &= \frac{\Gamma(b_1)\Gamma(b_2)\Gamma(b_3)}{2\sqrt{\pi}\Gamma(a_1)\Gamma(a_2)} (-z)^\chi \left( \exp(-i(\pi\chi + 2\sqrt{-z})) + \exp(i(\pi\chi + 2\sqrt{-z})) + \mathcal{O}\left(\frac{1}{\sqrt{-z}}\right) \right) \\ &+ \frac{\Gamma(b_1)\Gamma(b_2)\Gamma(b_3)\Gamma(a_2-a_1)}{\Gamma(b_1-a_1)\Gamma(b_2-a_1)\Gamma(b_3-a_1)\Gamma(a_2)} (-z)^{-a_1} \left( 1 + \mathcal{O}\left(\frac{1}{z}\right) \right) \\ &+ \frac{\Gamma(b_1)\Gamma(b_2)\Gamma(b_3)\Gamma(a_1-a_2)}{\Gamma(b_1-a_2)\Gamma(b_2-a_2)\Gamma(b_3-a_2)\Gamma(a_1)} (-z)^{-a_2} \left( 1 + \mathcal{O}\left(\frac{1}{z}\right) \right) \quad (\text{A.55}) \end{aligned}$$

at  $\chi = \frac{1}{2}(a_1 + a_2 - b_1 - b_2 - b_3 + \frac{1}{2})$  and wherein the case of simple poles (i.e.  $a_1 - a_2 \notin \mathbb{Z}$ ).

After some long but simple calculations using the properties Eq.(A.53), Eq.(A.54) and Eq.(A.55), an integral in Eq.(A.52) is shown

$$\int_{\epsilon}^{b^{\Delta}} dx x^{\frac{3-\Delta}{2}} K_{\frac{1}{2\Delta}-1}(x) K_{\frac{1}{2\Delta}+1}(x) = -\frac{3\sqrt{\pi}\Gamma(1+\frac{1}{\Delta})\Gamma(\frac{3}{2\Delta}-1)\Gamma(\frac{2}{\Delta})}{8\Gamma(\frac{\Delta+3}{2\Delta})} + \frac{\pi\epsilon^{3-2\Delta}}{2(3-2\Delta)} \csc\left(\frac{\pi}{2\Delta}\right) \quad (\text{A.56})$$

with  $b \rightarrow \infty$ . Substitute Eq.(A.56) into Eq.(A.52), and we have

$$F_{\Delta}(b) = \frac{\pi b^{3-2\Delta}}{4\Delta^2(3-2\Delta)} \csc\left(\frac{\pi}{2\Delta}\right) - \frac{\sqrt{\pi}\Gamma(\frac{3}{2\Delta}-1)\Gamma(\frac{1}{\Delta})\Gamma(\frac{2}{\Delta})}{8\Delta^2\Gamma(\frac{\Delta+3}{2\Delta})} \quad (\text{A.57})$$

Putting Eq.(A.48) and Eq.(A.57) into Eq.(A.44), we have

$$g^2 \mathcal{A}^2 = \frac{b^2}{-\frac{\sqrt{\pi}\Gamma(\frac{3}{2\Delta}-1)\Gamma(\frac{1}{\Delta})\Gamma(\frac{2}{\Delta})}{8\Delta^2\Gamma(\frac{\Delta+3}{2\Delta})} + \frac{\pi(3-\Delta)^2 \csc(\frac{\pi}{2\Delta})}{4\Delta^4(3-2\Delta)}} b^{3-2\Delta} \quad (\text{A.58})$$

Apply Eq.(A.51) into Eq.(A.41) using Eq.(2.4), we deduce

$$\frac{\rho}{r_h^2} = -\frac{\Gamma(\frac{-1}{2\Delta})}{2^{1+\frac{1}{2\Delta}}} \mathcal{A} b \quad (\text{A.59})$$

As we combine  $T_c = \frac{3}{4\pi} r_c = \frac{3}{4\pi} \sqrt{\frac{\rho}{\lambda_3}}$ , Eq.(A.27), Eq.(A.58) and Eq.(A.59) with  $b = \left(\frac{g\langle\mathcal{O}_{\Delta}\rangle}{\Delta r_h^{\Delta}}\right)^{\frac{1}{\Delta}}$  in the form of  $X$ ; here,  $X := \frac{g^{1/\Delta}\langle\mathcal{O}_{\Delta}\rangle^{1/\Delta}}{T_c}$  for simple notation, we obtain the condensate at  $T \approx 0$ :

$$X^4 = G_3^4 (\alpha_3 + \beta_3 \tau_3^{3-2\Delta} X^{3-2\Delta}) \quad (\text{A.60})$$

$$\begin{aligned} \text{where } G_3 &= \frac{4\pi\Delta^{1/\Delta}}{3} \left(\frac{-2^{1+\nu}\lambda_{g,3}}{\Gamma(-\nu)}\right)^{\frac{1}{2}} \\ \alpha_3 &= -\frac{\sqrt{\pi}\Gamma(\frac{3-2\Delta}{2\Delta})\Gamma(\frac{1}{\Delta})\Gamma(\frac{2}{\Delta})}{8\Delta^2\Gamma(\frac{3+\Delta}{2\Delta})} \\ \beta_3 &= \frac{\nu\pi(3-\Delta)^2 \csc(\nu\pi)}{2\Delta^3(3-2\Delta)}. \end{aligned} \quad (\text{A.61})$$

with  $\nu = \frac{1}{2\Delta}$  and  $\tau_3 = \frac{3}{4\pi\Delta^{1/\Delta}} \frac{T_c}{T}$ .

The authors of ref. [8] argued that  $X$  approaches to zero as  $\Delta \rightarrow 3$ , while Horowitz et.al [7]'s numerical calculation got a finite value  $X = 8.8$  at  $\Delta = 3$  (see FIG. 14). On the other hand, our calculation show  $X = 7.2$  at  $\Delta = 3$ . Our result is good agreement with the one of ref [7].

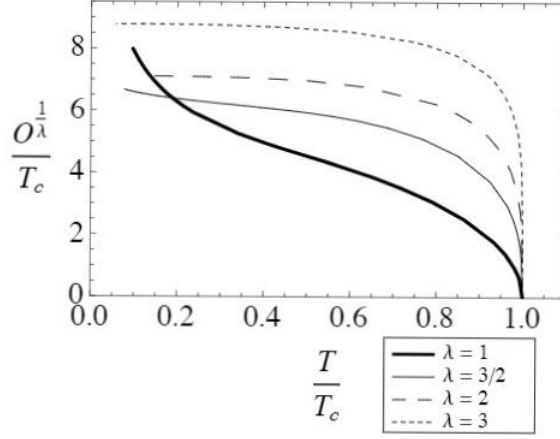


**Figure 14:** Result of ref. [7]: The condensate as a function of temperature. Here,  $\lambda = \Delta$ .

### A.2.2 Analytic calculation of $g^{\frac{1}{\Delta}} \frac{\langle \mathcal{O}_\Delta \rangle^{\frac{1}{\Delta}}}{T_c}$ at $\Delta = 3/2$

$\alpha_3$  and  $\beta_3$  in Eq.(A.61) have series expansions at  $\Delta = 3/2$ :

$$\alpha_3 = \frac{\pi \csc\left(\frac{2\pi}{3}\right)}{18\left(\Delta - \frac{3}{2}\right)} + \frac{\pi \csc\left(\frac{2\pi}{3}\right) \left(3 + 3(-\log(4)) - 4\psi\left(2 - \frac{2}{3}\right) - 2\psi\left(\frac{2}{3}\right)\right)}{3^4} + \mathcal{O}\left(\Delta - \frac{3}{2}\right) \quad (\text{A.62})$$

$$\beta_3 = -\frac{\pi \csc\left(\frac{2\pi}{3}\right)}{18\left(\Delta - \frac{3}{2}\right)} + \frac{\pi \left(18 + \pi \cot\left(\frac{2\pi}{3}\right)\right) \csc\left(\frac{2\pi}{3}\right)}{3^4} + \mathcal{O}\left(\Delta - \frac{3}{2}\right). \quad (\text{A.63})$$

As Eq.(A.62) and Eq.(A.63) are substituted into Eq.(A.60) with taking the limit  $\Delta \rightarrow 3/2$ , we obtain

$$X^4 = G_3^4 \left( \rho_3 + \frac{\sigma_3}{2} \left( \frac{1 - \tau_3^{3-2\Delta} X^{3-2\Delta}}{\Delta - \frac{3}{2}} \right) \right) \quad (\text{A.64})$$

where

$$\begin{aligned} \sigma_3 &= \frac{\pi \csc\left(\frac{2\pi}{3}\right)}{9} \\ \rho_3 &= \frac{\sigma_3}{3} \left( 21 - 3\ln(4) + \pi \cot\left(\frac{2\pi}{3}\right) - 4\psi\left(\frac{4}{3}\right) - 2\psi\left(\frac{2}{3}\right) \right) \\ &= \frac{\sigma_3}{3} \left( 3 - \pi \cot\left(\frac{2\pi}{3}\right) - \ln(4) - 2\psi\left(\frac{2}{3}\right) \right) \end{aligned}$$

here,  $\psi(z)$  is the digamma function. By using L'Hopital's rule, Eq.(A.64) becomes

$$\begin{aligned} X^4 &= G_3^4 \left( \rho_3 - \frac{\sigma_3}{2} \frac{\partial}{\partial \Delta} \left( \tau_3^{3-2\Delta} X^{3-2\Delta} \right) \right) \\ &= G_3^4 (\rho_3 + \sigma_3 \ln(\tau_3 X)) \end{aligned} \quad (\text{A.65})$$

Fig. 15 (b) tells us that  $X \sim \ln(T_c/T)^{1/4}$  for low temperature; Numerical result tells us that  $X^4 - \log(T/T_c)$  plot demonstrates our arguments with high precision.

And  $X$  is numerically

$$X \approx 6.76 \left( 1 + 0.45 \ln \left( \frac{T_c}{T} \right) \right)^{1/4} \quad (\text{A.66})$$

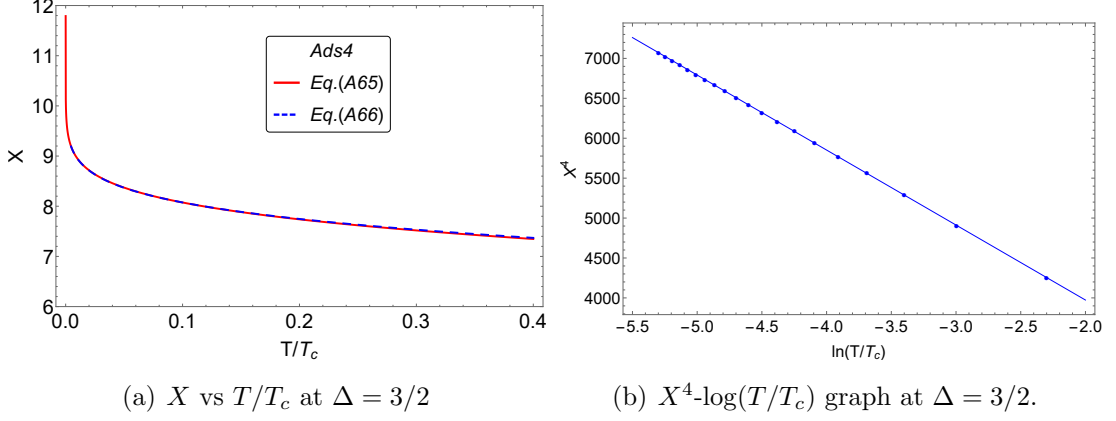


**Figure 15:** (a)  $X$  vs  $T/T_c$ : red colored curves for  $X$  is a plot of Eq.(A.65). And blue curves is a plot of Eq.(A.66). These two curves are almost indetical for low temperature. (b)  $X^4$ - $\log(T/T_c)$  graph at  $\Delta = 3/2$ : The slope of blue dotted line for  $X^4$  is  $-939$ .

### A.3 Maxwell perturbations and the conductivity at near the zero temperature

The Maxwell equation at zero spatial momentum and with a time dependence of the form  $e^{-i\omega t}$  gives

$$r_+^2 (1 - z^3)^2 \frac{d^2 A_x}{dz^2} - 3r_+^2 z^2 (1 - z^3) \frac{dA_x}{dz} + (\omega^2 - V(z)) A_x = 0$$

where  $A_x$  is any component of the perturbing electromagnetic potential along the boundary and

$$V(z) = \frac{g^2 \langle \mathcal{O}_\Delta \rangle^2}{r_+^{2\Delta-2}} (1 - z^3) z^{2\Delta-2} F(z)^2$$

with  $F$  defined before. We introduce  $A_x(z) = (1 - z^3)^{-\frac{i}{3}\hat{\omega}} G(z)$  where  $\hat{\omega} = \omega/r_+$ . Because we require  $A_x \propto (1 - z^3)^{-\frac{i}{3}\hat{\omega}}$  near  $z = 1$  corresponding to ingoing wave boundary conditions at the horizon. Then, the wave equation reads

$$(1 - z^3) \frac{d^2 G}{dz^2} - 3 \left( 1 - \frac{2i\hat{\omega}}{3} \right) z^2 \frac{dG}{dz} + \left( \frac{\hat{\omega}^2 (1+z)(1+z^2)}{1+z+z^2} + 2i\hat{\omega}z - \frac{g^2 \langle \mathcal{O}_\Delta \rangle^2}{r_+^{2\Delta}} z^{2\Delta-2} F^2(z) \right) G = 0$$

We have the following limiting form:

$$\lim_{z \rightarrow 0} K_\nu(z) \sim \frac{\Gamma(\nu)}{2} \left( \frac{z}{2} \right)^{-\nu} \sum_{k=0}^1 \frac{\left( \frac{z}{2} \right)^{2k}}{(1-\nu)_k k!} + \frac{\Gamma(-\nu)}{2} \left( \frac{z}{2} \right)^\nu \sum_{k=0}^1 \frac{\left( \frac{z}{2} \right)^{2k}}{(1+\nu)_k k!} \quad (\text{A.67})$$

at  $\nu \neq \mathbb{Z}$ .

We obtain the analytic expressions of  $F(z)$  in the following way:

$$F(z) \approx 1 - \frac{(bz)^4 \mathbb{J}_1 + (bz)^3 \mathbb{J}_2 + (bz)^2 \mathbb{J}_3}{-\frac{\sqrt{\pi}\Gamma(\frac{3}{2\Delta}-1)\Gamma(\frac{1}{\Delta})\Gamma(\frac{2}{\Delta})}{8\Delta^2\Gamma(\frac{\Delta+3}{2\Delta})} + \frac{\pi(3-\Delta)^2 \csc(\frac{\pi}{2\Delta})}{4\Delta^4(3-2\Delta)} b^{3-2\Delta}}, \quad \text{for } z \leq 1/b, \quad (\text{A.68})$$

$$F(z) \approx 1 - \frac{-\frac{\sqrt{\pi}\Gamma(\frac{3}{2\Delta}-1)\Gamma(\frac{1}{\Delta})\Gamma(\frac{2}{\Delta})}{8\Delta^2\Gamma(\frac{\Delta+3}{2\Delta})} + \frac{\pi \csc(\frac{\pi}{2\Delta})}{4\Delta^2(3-2\Delta)} (bz)^{3-2\Delta}}{-\frac{\sqrt{\pi}\Gamma(\frac{3}{2\Delta}-1)\Gamma(\frac{1}{\Delta})\Gamma(\frac{2}{\Delta})}{8\Delta^2\Gamma(\frac{\Delta+3}{2\Delta})} + \frac{\pi(3-\Delta)^2 \csc(\frac{\pi}{2\Delta})}{4\Delta^4(3-2\Delta)} b^{3-2\Delta}}, \quad \text{for } z > 1/b. \quad (\text{A.69})$$

where

$$\begin{aligned} \mathbb{J}_1 &= 2^{-\frac{1}{\Delta}-8}\Gamma\left(-1 - \frac{1}{2\Delta}\right)^2 \left(\frac{8\Delta+4}{\Delta^2} + \frac{8(2\Delta+1)(bz)^{2\Delta}}{\Delta(4\Delta^2+9\Delta+2)} + \frac{(bz)^{4\Delta}}{6\Delta^2+7\Delta+1}\right) \\ \mathbb{J}_2 &= -\frac{1}{24}\pi \csc\left(\frac{\pi}{2\Delta}\right) \left(\frac{\Delta^2(48\Delta+(2\Delta+3)(bz)^{2\Delta}+36)}{(2\Delta+3)(4\Delta+3)(4\Delta^2-1)} + 4\right) \\ \mathbb{J}_3 &= 2^{\frac{1}{\Delta}-7}\Gamma\left(\frac{1}{2\Delta}-1\right)^2 \left(\frac{8\Delta-4}{\Delta^2} + \frac{4(2\Delta-1)(bz)^{2\Delta}}{\Delta(4\Delta^2+3\Delta-1)} + \frac{(bz)^{4\Delta}}{12\Delta^2+4\Delta-1}\right) \end{aligned} \quad (\text{A.70})$$

As we apply Eq.(A.67) and Eq.(A.58) into Eq.(A.43a), we obtain Eq.(A.68).

Replacing  $b$  by  $bz$  in Eq.(A.45a) and Eq.(A.57), we have

$$\begin{aligned} F_\Delta(bz) &= \int_0^{bz} dz z^{2-2\Delta} \int_0^z d\tilde{z} \tilde{z}^{2\Delta-1} \left(K_{\frac{1}{2\Delta}}(\tilde{z}^\Delta)\right)^2 \\ &= b^3 \int_0^z dz z^{2-2\Delta} \int_0^z d\tilde{z} \tilde{z}^{2\Delta-1} \left(K_{\frac{1}{2\Delta}}(b^\Delta \tilde{z}^\Delta)\right)^2 \\ &= \frac{\pi \csc\left(\frac{\pi}{2\Delta}\right)}{4\Delta^2(3-2\Delta)} (bz)^{3-2\Delta} - \frac{\sqrt{\pi}\Gamma\left(\frac{3}{2\Delta}-1\right)\Gamma\left(\frac{1}{\Delta}\right)\Gamma\left(\frac{2}{\Delta}\right)}{8\Delta^2\Gamma\left(\frac{\Delta+3}{2\Delta}\right)} \end{aligned} \quad (\text{A.71})$$

Substitute Eq.(A.71) and Eq.(A.58) into Eq.(A.43a). We obtain Eq.(A.69).

Fig. 16 shows how the data fits by above formulas Eq.(A.68) and Eq.(A.69).

$F(z) \approx 1$  at  $\Delta = 1$  in Eq.(A.68) and Eq.(A.69). And the solution of Eq.(5.5) is

$$G(z) = \exp\left(iz\sqrt{\hat{\omega}^2 - \frac{g^2 \langle \mathcal{O}_1 \rangle^2}{r_+^2}}\right) + R \exp\left(-iz\sqrt{\hat{\omega}^2 - \frac{g^2 \langle \mathcal{O}_1 \rangle^2}{r_+^2}}\right) \quad (\text{A.72})$$

Here,  $R$  is a reflection coefficient.  $T \rightarrow 0$  is equivalent to sending the horizon to infinity. Then infalling boundary condition corresponds to  $R = 0$ . Then it gives the conductivities to be

$$\sigma(\omega) = \frac{\sqrt{\omega^2 - g^2 \langle \mathcal{O}_1 \rangle^2}}{\omega} \quad (\text{A.73})$$

via Eq.(5.4).

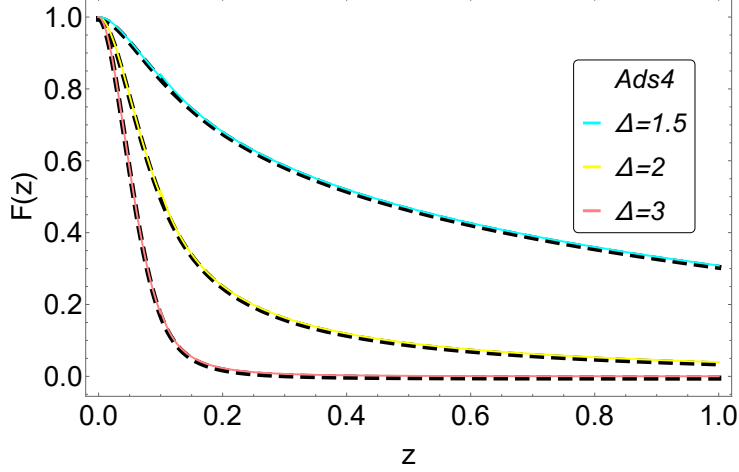


**Figure 16:** The field  $F$  for  $\Delta = 1.5$  (light blue),  $\Delta = 2$  (yellow),  $\Delta = 3$  (pink) at  $b = 10$ . Solid colored curves are analytic expression Eq.(A.68) and Eq.(A.69) and dashed curves are exact numerical results Eq.(A.43a) with Eq.(A.58) (almost indistinguishable).

For  $\Delta = 2$  in Eq.(5.5), We may substitute the trial function

$$F(z) = \frac{\tanh(1.5bz)}{1.5bz} \quad (\text{A.74})$$

which is satisfied with Eq.(A.68) and Eq.(A.69) numerically. Also, this trial function obey the correct boundary conditions ( $F(0) = 1$ ,  $F'(0) = 1$  and  $\lim_{z \rightarrow \infty} F(z) \propto (bz)^{3-2\Delta}$ ). Here,  $b = \frac{\sqrt{g\langle \mathcal{O}_2 \rangle}}{\sqrt{2}r_+}$ . Then at low temperature Eq.(5.5) reads

$$\frac{d^2 G}{dz^2} + (\hat{\omega}^2 - b^2 \tanh^2(2bz)) G = 0 \quad (\text{A.75})$$

whose general solution is given in terms of Legendre functions,

$$G(z) = P_\nu^\mu(\tanh(1.5bz)) + R P_\nu^{-\mu}(\tanh(1.5bz)) \quad (\text{A.76})$$

where  $\nu = \frac{-9+\sqrt{337}}{18}$  and  $\mu = \frac{2i\sqrt{\hat{\omega}^2 - (\frac{4}{3}b)^2}}{3b}$ . Similar to  $\Delta = 1$ , we choose infalling boundary condition corresponds to  $R = 0$ . This exact result then produces the nonzero conductivities

$$\sigma(\omega) = \frac{3i\sqrt{g\langle \mathcal{O}_2 \rangle}}{\sqrt{2}\omega} \frac{\Gamma\left(\frac{1}{36}\left(27 - \sqrt{337} - 16i\sqrt{P(\omega)}\right)\right) \Gamma\left(\frac{1}{36}\left(27 + \sqrt{337} - 16i\sqrt{P(\omega)}\right)\right)}{\Gamma\left(\frac{1}{36}\left(9 - \sqrt{337} - 16i\sqrt{P(\omega)}\right)\right) \Gamma\left(\frac{1}{36}\left(9 + \sqrt{337} - 16i\sqrt{P(\omega)}\right)\right)} \quad (\text{A.77})$$

via Eq.(5.4) where

$$P(\omega) = \frac{9}{8} \frac{\omega^2}{g\langle \mathcal{O}_2 \rangle} - 1.$$

Here we apply the following limiting form:

$$\lim_{z \rightarrow 0} P_\nu^\mu(z) = \frac{2^\mu \sqrt{2}}{\Gamma\left(1 + \frac{\nu}{2} - \frac{\mu}{2}\right) \Gamma\left(\frac{1}{2} - \frac{\nu}{2} - \frac{\mu}{2}\right)} \quad (\text{A.78})$$

The solution of Eq.(5.11) is

$$G_0(z) = \sqrt{bz} K_{\frac{1}{2\Delta}}(b^\Delta z^\Delta) + R \sqrt{bz} I_{\frac{1}{2\Delta}}(b^\Delta z^\Delta) \quad (\text{A.79})$$

Here, we take  $R = 0$ : The other solution  $\sqrt{bz} I_{\frac{1}{2\Delta}}(b^\Delta z^\Delta)$  is rejected because it is monotonically increasing as  $z$  increases for large  $b$ . By substituting Eq.(A.79), the solution to the field equation Eq.(5.12) for  $G_1$  is

$$\begin{aligned} G_1(z) = & \sqrt{bz} K_{\frac{1}{2\Delta}}(b^\Delta z^\Delta) \\ & + \frac{i\sqrt{b}}{6} z^{7/2} \left\{ 2\pi \csc\left(\frac{\pi}{2\Delta}\right) \left( I_{-\frac{1}{2\Delta}}(b^\Delta z^\Delta) + I_{\frac{1}{2\Delta}}(b^\Delta z^\Delta) \right) {}_2F_3 \left[ 1 - \frac{1}{2\Delta}, 1 + \frac{1}{2\Delta}, 1 + \frac{3}{2\Delta}; b^{2\Delta} z^{2\Delta} \right] \right. \\ & - 6\Delta \frac{2^{1/\Delta}}{\sqrt{bz}} \left( \Gamma\left(1 + \frac{1}{2\Delta}\right) \right)^2 I_{\frac{1}{2\Delta}}(b^\Delta z^\Delta) {}_2F_3 \left[ 1 - \frac{1}{\Delta}, 1 - \frac{1}{2\Delta}, 1 + \frac{1}{\Delta}; b^{2\Delta} z^{2\Delta} \right] \\ & \left. - 3\Delta \frac{\sqrt{bz}}{2^{1/\Delta}} \left( \Gamma\left(1 - \frac{1}{2\Delta}\right) \right)^2 I_{-\frac{1}{2\Delta}}(b^\Delta z^\Delta) {}_2F_3 \left[ 1 + \frac{1}{\Delta}, 1 + \frac{1}{2\Delta}, 1 + \frac{2}{\Delta}; b^{2\Delta} z^{2\Delta} \right] \right\} \quad (\text{A.80}) \end{aligned}$$

Eq.(A.79) and Eq.(A.80) give us the nonzero conductivities

$$\lim_{\omega \rightarrow 0} \sigma(\omega) = \frac{2\pi\Delta \csc\left(\frac{\pi}{2\Delta}\right) g^{1/\Delta} \langle \mathcal{O}_\Delta \rangle^{1/\Delta}}{(2\Delta)^{1/\Delta} \left( \Gamma\left(\frac{1}{2\Delta}\right) \right)^2 \omega} i \quad (\text{A.81})$$

And we obtain

$$\frac{n_s}{T_c} = \frac{2\pi\Delta \csc\left(\frac{\pi}{2\Delta}\right) g^{1/\Delta} \langle \mathcal{O}_\Delta \rangle^{1/\Delta}}{(2\Delta)^{1/\Delta} \left( \Gamma\left(\frac{1}{2\Delta}\right) \right)^2 T_c} \quad (\text{A.82})$$

here,  $n_s$  is also the coefficient of the pole in the imaginary part  $\text{Im}\sigma(\omega) \sim n_s/\omega$  as  $\omega \rightarrow 0$ .

#### A.4 Expression for the schrödinger wave equation of the conductivity at near the zero temperature

Eq.(5.1) takes the form of a schrödinger equation with energy  $\omega$ :

$$-\frac{d^2 A_x}{dr_\star^2} + V(r_\star) A_x = \omega^2 A_x.$$

Here,  $V(r_\star)$  is re-expression of  $V(z) = \frac{g^2 \langle \mathcal{O}_\Delta \rangle^2}{r_+^{2\Delta-2}} (1-z^3) z^{2\Delta-2} F(z)^2$  in terms of the tortoise coordinate  $r_\star$ ,

$$r_\star = \int \frac{dr}{f(r)} = \frac{1}{6r_+} \left[ \ln \frac{(1-z)^3}{1-z^3} - 2\sqrt{3} \tan^{-1} \frac{\sqrt{3}z}{2+z} \right],$$

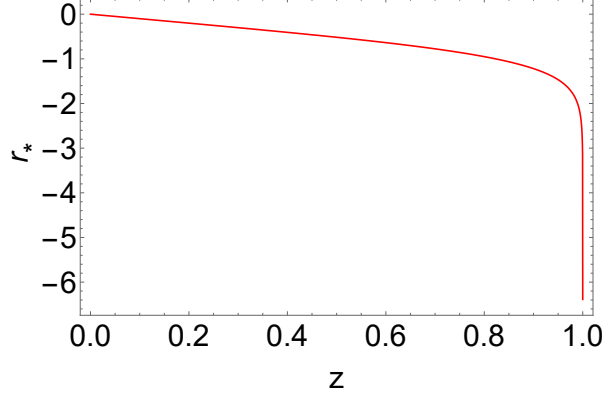


**Figure 17:**  $r_*$  vs  $z$  Here,  $r_+ = 1$  for simplicity.

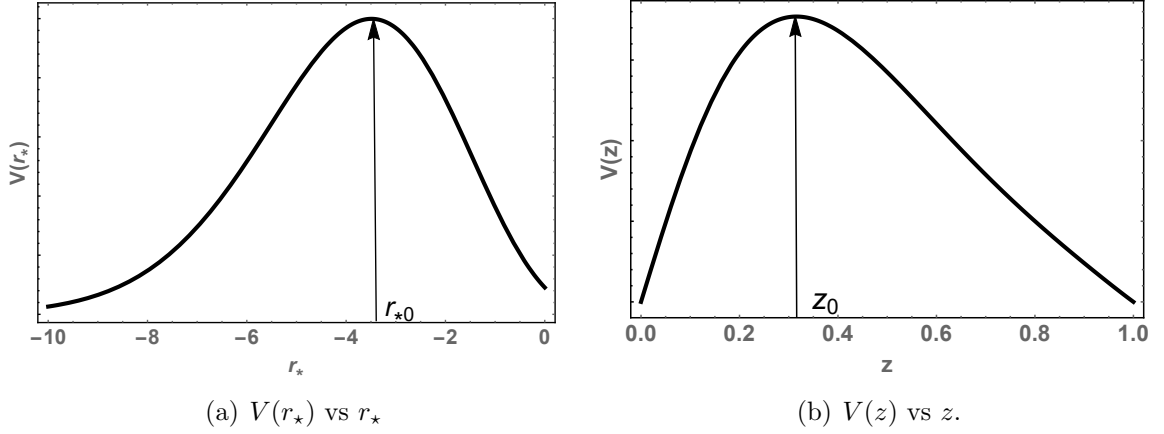


**Figure 18:** (a) a rough picture  $V(r_*)$  in terms of a  $r_*$  coordinate, (b) a rough picture  $V(z)$  in terms of a  $z$  coordinate.

where the integration constant is chosen such that boundary is at  $r_* = 0$ .

FIG. 17. shows that the horizon corresponds to  $r_* = -\infty$ . We can easily show that  $V(r_* = 0) = 0$  if  $\Delta > 1$ ,  $V(r_* = 0)$  is a nonzero constant if  $\Delta = 1$ , and  $V(r_*)$  diverges as  $r_* \rightarrow 0$  if  $1/2 < \Delta < 1$ . FIG. 18. can show that  $V(z)$  always vanishes at the horizon (or  $V(r_*)$  vanishes at  $r_* \rightarrow -\infty$ ). The maximum value of  $V(r_*)$  (or  $V(z)$ ) always exists at  $r_* = r_{*0}$  (or  $z = z_0$ ) if  $\Delta \geq 1$ . As we substitute Eq.(A.69) into Eq.(5.16), we obtain a polynomial equation such as

$$z_0^{2\Delta}(3 - \Delta)^2(2 + z_0^3 + 2\Delta(z_0^3 - 1)) + \Delta^2 z_0^3(4 - 2\Delta + (2\Delta - 7)z_0^3) = 0. \quad (\text{A.83})$$

And its numerical solution is

$$z_0 \approx 0.41249 \sum_{k=1}^{\infty} \frac{\sin(\pi(\Delta - 1)(2k - 1))}{k^{2.6376}} \quad (\text{A.84})$$

where  $1 \leq \Delta < 2$ . A dashed curve at  $1 \leq \Delta < 2$  in FIG. 8 (a). indicates Eq.(A.84), and we see that there are no  $b$  (or  $T$ ) dependence.

As we substitute Eq.(A.68) into Eq.(5.16), we obtain a polynomial equation, and we see  $z_0 \propto 1/b$ . Its numerical solution is

$$z_0 \approx \left( \frac{0.1}{\Delta - 1.83} + 0.7 \right) \frac{1}{b} \quad (\text{A.85})$$

where  $2 \leq \Delta \leq 3$ . A dashed curve at  $2 \leq \Delta \leq 3$  in FIG. 8. indicates Eq.(A.85), and we see that there are  $b$  dependence.

And  $\omega_g$  is given by

$$\omega_g = \sqrt{V_{\max}} = \frac{g \langle \mathcal{O}_\Delta \rangle}{r_+^{\Delta-1}} \sqrt{1 - z_0^3 z_0^{\Delta-1} F(z_0)} \approx \frac{g \langle \mathcal{O}_\Delta \rangle}{r_+^{\Delta-1}} z_0^{\Delta-1} F(z_0). \quad (\text{A.86})$$

We obtain the analytic expressions of  $\frac{\omega_g}{T_c}$  in the following way:

$$\frac{\omega_g}{T_c} = \left( \frac{3z_0 T_c}{4\pi T} \right)^{\Delta-1} \left( \frac{g^{1/\Delta} \langle \mathcal{O}_\Delta \rangle^{1/\Delta}}{T_c} \right)^\Delta F_{<}(z_0), \quad \text{for } 1 \leq \Delta < 2, \quad (\text{A.87})$$

$$\frac{\omega_g}{T_c} = (\Delta^{1/\Delta} \rho_\Delta)^{\Delta-1} \frac{g^{1/\Delta} \langle \mathcal{O}_\Delta \rangle^{1/\Delta}}{T_c} F_{>}(\rho_\Delta), \quad \text{for } 2 \leq \Delta \leq 3, \quad (\text{A.88})$$

where

$$F_{<}(z_0) = 1 - \frac{-\frac{\sqrt{\pi}\Gamma(\frac{3}{2\Delta}-1)\Gamma(\frac{1}{\Delta})\Gamma(\frac{2}{\Delta})}{8\Delta^2\Gamma(\frac{\Delta+3}{2\Delta})} + \frac{\pi \csc(\frac{\pi}{2\Delta})}{4\Delta^2(3-2\Delta)}(bz_0)^{3-2\Delta}}{-\frac{\sqrt{\pi}\Gamma(\frac{3}{2\Delta}-1)\Gamma(\frac{1}{\Delta})\Gamma(\frac{2}{\Delta})}{8\Delta^2\Gamma(\frac{\Delta+3}{2\Delta})} + \frac{\pi(3-\Delta)^2 \csc(\frac{\pi}{2\Delta})}{4\Delta^4(3-2\Delta)}b^{3-2\Delta}}, \quad (\text{A.89})$$

$$F_{>}(\rho_\Delta) = 1 + \frac{\Delta^2 \rho_\Delta^2 \Gamma(\frac{3+\Delta}{2\Delta}) [\rho_\Delta \mathbb{M}_1 + \rho_\Delta^2 \mathbb{M}_2 + \mathbb{M}_3]}{6\sqrt{\pi}\Gamma(\frac{1}{\Delta})\Gamma(\frac{2}{\Delta})\Gamma(-1+\frac{3}{2\Delta})}, \quad (\text{A.90})$$

with

$$\begin{aligned} \mathbb{M}_1 &= 8\pi \csc\left(\frac{\pi}{2\Delta}\right) \left( -1 + \frac{3\Delta^2 \rho_\Delta^{2\Delta}}{3 - 2\Delta(4\Delta^2 + 6\Delta - 1)} \right), \\ \mathbb{M}_2 &= \frac{3 \left( \Gamma\left(\frac{-1}{2\Delta}\right) \right)^2}{2^{1/\Delta}} \left( \frac{2 + \Delta(9 + 4\Delta + 2\rho_\Delta^{2\Delta})}{(2 + \Delta)(1 + 2\Delta)(1 + 4\Delta)} \right), \\ \mathbb{M}_3 &= 6 \left( \Gamma\left(\frac{1}{2\Delta}\right) \right)^2 2^{1/\Delta} \left( \frac{4\Delta^2 - 1 + \Delta(3 + \rho_\Delta^{2\Delta})}{8\Delta^3 + 2\Delta^2 - 5\Delta + 1} \right), \\ \rho_\Delta &= \left( \frac{0.1}{\Delta - 1.83} + 0.7 \right). \end{aligned} \quad (\text{A.91})$$

Substitute Eq.(A.69) with Eq.(A.84) into Eq.(A.86) and we obtain Eq.(A.87). Also, substitute Eq.(A.68) with Eq.(A.85) into Eq.(A.86) and we obtain Eq.(A.88). A numerical result tells us that Eq.(A.88) approximately is

$$\frac{\omega_g}{T_c} \approx \frac{1.1}{\text{li}(\Delta^{1.2})} \frac{g^{1/\Delta} \langle \mathcal{O}_\Delta \rangle^{1/\Delta}}{T_c}, \quad (\text{A.92})$$

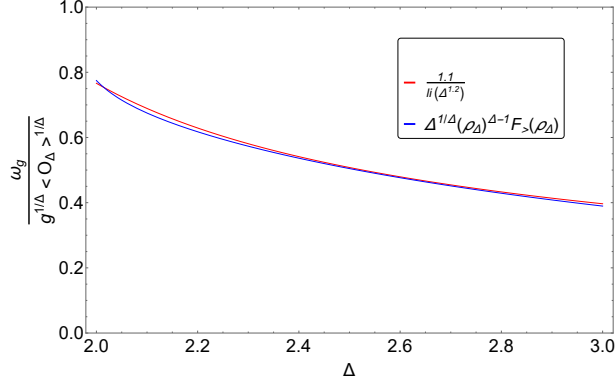


**Figure 19:** Solid red curve is a plot of  $\frac{1.1}{\text{li}(\Delta^{1.2})}$  and blue one is a plot of  $(\Delta^{1/\Delta}\rho_\Delta)^{\Delta-1} F_{>}(\rho_\Delta)$  with Eq.(A.90) in Eq.(A.88) (almost indistinguishable).

here,  $\text{li}(x)$  is an logarithmic integral function. See Fig.19.

And we can classify Eq.(A.87) into the following way:

1. As  $1 \leq \Delta \ll 3/2$ ,

$$\frac{\omega_g}{T_c} = \left( \frac{3z_0 T_c}{4\pi T} \right)^{\Delta-1} \left( 1 - \left( \frac{\Delta}{3-\Delta} z_0^{3/2-\Delta} \right)^2 \right) X^\Delta \quad (\text{A.93})$$

2. As  $\Delta = 3/2$ ,

$$\frac{\omega_g}{T_c} = \frac{7}{10} \frac{X^{3/2} \left( \frac{T_c}{T} \right)^{1/2}}{\ln \left( X \frac{T_c}{T} \right)} \quad (\text{A.94})$$

3. As  $3/2 \ll \Delta < 2$ ,

$$\frac{\omega_g}{T_c} = \left( \frac{3z_0 T_c}{4\pi T} \right)^{2-\Delta} \frac{\sqrt{\pi} \Gamma \left( \frac{3+\Delta}{2+\Delta} \right) \csc \left( \frac{\pi}{2\Delta} \right)}{\Delta^{3/\Delta} \Gamma \left( \frac{2}{\Delta} \right) \Gamma \left( \frac{3}{2\Delta} \right) \Gamma \left( 1 + \frac{1}{\Delta} \right)} \left( 1 - \left( \frac{\Delta}{3-\Delta} z_0^{\Delta-3/2} \right)^2 \right) X^{3-\Delta} \quad (\text{A.95})$$

Here,  $X = \frac{g^{1/\Delta} (\mathcal{O}_\Delta)^{1/\Delta}}{T_c}$ .

From Eq.(A.82), Eq.(A.93), Eq.(A.94) and Eq.(A.95), we find a relation between  $n_s$  and the gap frequency  $\omega_g$ :

1. As  $1 \leq \Delta \ll 3/2$ ,

$$\frac{n_s}{\omega_g} = \frac{2\pi\Delta \csc \left( \frac{\pi}{2\Delta} \right)}{(2\Delta)^{1/\Delta} \left( \Gamma \left( \frac{1}{2\Delta} \right) \right)^2} \frac{1}{1 - \left( \frac{\Delta}{3-\Delta} z_0^{3/2-\Delta} \right)^2} \left( \frac{3z_0}{4\pi} X \right)^{1-\Delta} \quad (\text{A.96})$$

2. As  $\Delta = 3/2$ ,

$$\frac{n_s}{\omega_g} = \frac{\ln \left( X \frac{T_c}{T} \right)}{\sqrt{X \frac{T_c}{T}}} \quad (\text{A.97})$$

3. As  $3/2 \ll \Delta < 2$ ,

$$\frac{n_s}{\omega_g} = \frac{2\sqrt{\pi}\Delta^{1+3/\Delta}}{(2\Delta)^{1/\Delta} \left(\Gamma\left(\frac{1}{2\Delta}\right)\right)^2} \frac{\Gamma\left(\frac{2}{\Delta}\right) \Gamma\left(\frac{3}{2\Delta}\right) \Gamma\left(1 + \frac{1}{\Delta}\right)}{\Gamma\left(\frac{3+\Delta}{2\Delta}\right)} \frac{1}{1 - \left(\frac{\Delta}{3-\Delta} z_0^{\Delta-3/2}\right)^2} \left(\frac{3z_0}{4\pi} X\right)^{\Delta-2} \quad (\text{A.98})$$

4. As  $2 \leq \Delta \leq 3$ ,

$$\frac{n_s}{\omega_g} = \frac{2\pi\Delta \csc\left(\frac{\pi}{2\Delta}\right)}{1.1(2\Delta)^{1/\Delta} \left(\Gamma\left(\frac{1}{2\Delta}\right)\right)^2} \text{li}(\Delta^{1.2}) \quad (\text{A.99})$$

A numerical result tells us that Eq.(A.99) is approximately

$$\frac{n_s}{\omega_g} \approx 0.8\Delta - 0.7, \quad (\text{A.100})$$

here,  $z_0$  is Eq.(A.84). See Fig.20.

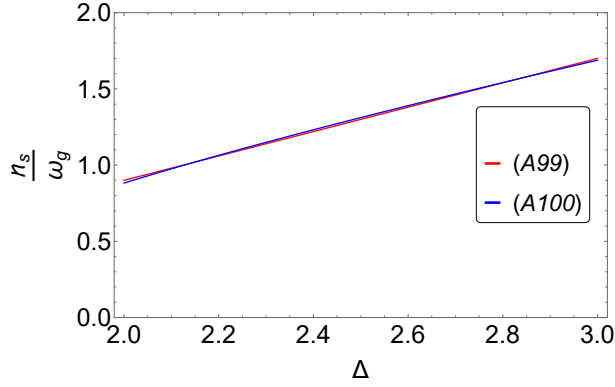


**Figure 20:** Solid red curve is a plot of Eq.(A.99) and blue one is a plot of Eq.(A.100) (almost indistinguishable).

As we see Fig 2. [7],  $\sigma(\omega)$  has a spike at  $\frac{\omega}{T_c} \approx 10.4$  and  $\Delta = 3/2$  for  $AdS_4$ . In FIG. 18 (b), resonance occurs well when the distance between  $z = 0$  and  $z = z_0$  is the maximum. FIG. 8 (a) shows that there is a maximum of  $z_0$  at  $\Delta = 3/2$ . So, the resonance, by which  $\sigma(\omega)$  diverges, occurs only in the vicinity of  $\Delta = 3/2$ . This can be understood using standard WKB matching formula: The resonance occurs when there exists  $\omega$  satisfying [14]

$$\int_{r_{*0}}^0 \sqrt{\omega^2 - V(r_*)} dr_* + \frac{\pi}{4} = n\pi, \quad (\text{A.101})$$

for an integer  $n$  and  $r_{*0} < 0$  is the position at which  $V$  has the maximum:  $\frac{dV}{dr_*}(r_{*0}) = 0$ . The above equation can be converted to  $z$  coordinate to give the following expression:

$$\frac{1}{r_+} \int_0^{z_0} \frac{\sqrt{\omega^2 - V(z)}}{1 - z^3} dz = \left(n - \frac{1}{4}\right) \pi. \quad (\text{A.102})$$

By applying Eq.(A.69) into Eq.(A.102), we obtain

$$\begin{aligned} \frac{1}{r_+} \int_0^{z_0} \frac{\sqrt{\omega^2 - V(z)}}{1 - z^3} dz &\approx \frac{1}{r_+} \int_{1/b}^{z_0} \frac{\sqrt{\omega^2 - \left(\frac{g\langle\mathcal{O}_\Delta\rangle}{r_+^{\Delta-1}}\right)^2 z^{2\Delta-2}(1-z^3) \left(\frac{(\beta-\beta_0 z^{3-2\Delta})b^{3-2\Delta}}{\alpha+\beta b^{3-2\Delta}}\right)^2}}{1 - z^3} dz \\ &\approx \frac{1}{r_+} \int_{1/b}^{z_0} \sqrt{\omega^2 - \left(\frac{g\langle\mathcal{O}_\Delta\rangle}{r_+^{\Delta-1}}\right)^2 z^{2\Delta-2} \left(\frac{(\beta-\beta_0 z^{3-2\Delta})b^{3-2\Delta}}{\alpha+\beta b^{3-2\Delta}}\right)^2} dz = \left(n - \frac{1}{4}\right) \pi, \end{aligned} \quad (\text{A.103})$$

where

$$\begin{aligned} \alpha &= -\frac{\sqrt{\pi}\Gamma\left(\frac{3}{2\Delta}-1\right)\Gamma\left(\frac{1}{\Delta}\right)\Gamma\left(\frac{2}{\Delta}\right)}{8\Delta^2\Gamma\left(\frac{\Delta+3}{2\Delta}\right)}, \\ \beta &= \frac{\pi(3-\Delta)^2 \csc\left(\frac{\pi}{2\Delta}\right)}{4\Delta^4(3-2\Delta)}, \\ \beta_0 &= \frac{\pi \csc\left(\frac{\pi}{2\Delta}\right)}{4\Delta^2(3-2\Delta)}. \end{aligned} \quad (\text{A.104})$$

At  $\Delta = 3/2$ , Eq.(A.103) becomes

$$\int_{1/b}^{z_0} \sqrt{\left(\frac{\omega}{T_c}\right)^2 - \left(\frac{2\pi T}{3 T_c}\right)^2 b^3 z \left(\frac{4-3\ln z}{2+\ln b}\right)^2} dz = \frac{4\pi^2}{3} \left(n - \frac{1}{4}\right) \frac{T}{T_c}, \quad (\text{A.105})$$

where  $z_0 = 0.362$  from Eq.(5.17), and

$$\begin{aligned} b &= 1.23 \left(1 + 0.45 \ln\left(\frac{T_c}{T}\right)\right)^{1/4} \frac{T_c}{T}, \\ \frac{\omega_g}{T_c} &= \frac{7}{10} \frac{X^{3/2} \left(\frac{T_c}{T}\right)^{1/2}}{\ln\left(X \frac{T_c}{T}\right)}, \quad \text{with } X = \frac{g^{1/\Delta} \langle\mathcal{O}_\Delta\rangle^{1/\Delta}}{T_c}. \end{aligned} \quad (\text{A.106})$$

Here, Eq.(A.106) is derived from Eq.(A.66).

Poles of $\sigma(\omega)$	$\frac{\omega_1}{T_c}$	$\frac{\omega_2}{T_c}$	$\frac{\omega_3}{T_c}$	$\frac{\omega_4}{T_c}$	$\frac{\omega_5}{T_c}$	$\frac{\omega_6}{T_c}$	$\frac{\omega_7}{T_c}$	$\frac{\omega_8}{T_c}$	$\frac{\omega_9}{T_c}$
$\frac{T}{T_c} = 0.1$ with $\omega_g/T_c = 10.9$	10.44								
$\frac{T}{T_c} = 0.05$ with $\omega_g/T_c = 13.4$	11.85	13.11							
$\frac{T}{T_c} = 0.04$ with $\omega_g/T_c = 14.62$	12.19	13.65	14.4						
$\frac{T}{T_c} = 0.03$ with $\omega_g/T_c = 16.34$	12.6	14.26	15.21	15.84	16.25				
$\frac{T}{T_c} = 0.02$ with $\omega_g/T_c = 19.18$	13.11	15.0	16.15	16.97	17.6	18.1	18.5	18.82	19.07

**Table 5:**  $\frac{\omega_n}{T_c}$  and  $\frac{T}{T_c}$  at lower  $T$ 's. where  $n = 1, 2, 3, \dots$ . A position of the pole is obtained from Eq.(A.105) with given  $\frac{T}{T_c}$  by applying Mathematica program.

## B Holographic superconductors with AdS<sub>5</sub>

### B.1 Near the critical temperature

#### B.1.1 Computation of $T_c$ by applying matrix algorithm and Pincherle's Theorem

At the critical temperature  $T_c$ ,  $\Psi = 0$ , so Eq.(2.3) tells us  $\Phi'' = 0$ . Then, we can set

$$\Phi(z) = \lambda_4 r_c (1 - x) \quad \text{where } \lambda_4 = \frac{\rho}{r_c^3} \quad (\text{B.1})$$

where  $x = z^2$ . As  $T \rightarrow T_c$ , the field equation  $\Psi$  approaches to

$$-\frac{d^2\Psi}{dx^2} + \frac{1+x^2}{x(1-x^2)} \frac{d\Psi}{dx} + \frac{m^2}{4x^2(1-x^2)} \Psi = \frac{\lambda_{g,4}^2}{4x(1+x)^2} \Psi \quad (\text{B.2})$$

where  $\lambda_{g,4} = g\lambda_4$ . Factoring out the behavior near the boundary  $z = 0$  and the horizon, we define

$$\Psi(x) = \frac{\langle \mathcal{O}_\Delta \rangle}{\sqrt{2}r_h^\Delta} x^{\frac{\Delta}{2}} F(x) \quad \text{where } F(x) = (1+x)^{-\lambda_{g,4}/2} y(x) \quad (\text{B.3})$$

Then,  $F$  is normalized as  $F(0) = 1$  and we obtain

$$\frac{d^2 y}{dx^2} + \left( \frac{\Delta-1}{x} + \frac{1}{x-1} + \frac{1-\lambda_{g,4}}{x+1} \right) \frac{dy}{dx} + \frac{\left( \frac{\Delta-\lambda_{g,4}}{4} x - \frac{\lambda_{g,4}}{2} \right) \left( \frac{\lambda_{g,4}}{2} - \Delta + 1 \right)}{x(x-1)(x+1)} y = 0. \quad (\text{B.4})$$

Eq.(B.4) is the Heun differential equation that has four regular singular points at  $z = 0, 1, -1, \infty$  [55]. Substituting  $y(x) = \sum_{n=0}^{\infty} d_n x^n$  into (B.4), we obtain the following three term recurrence relation:

$$\alpha_n d_{n+1} + \beta_n d_n + \gamma_n d_{n-1} = 0 \quad \text{for } n \geq 1, \quad (\text{B.5})$$

with

$$\begin{cases} \alpha_n = (n+1)(n+\Delta-1) \\ \beta_n = \frac{\lambda_{g,4}}{2} \left( 2n+\Delta-1 - \frac{\lambda_{g,4}}{2} \right) \\ \gamma_n = \left( n-1 + \frac{\Delta}{2} - \frac{\lambda_{g,4}}{2} \right)^2 \end{cases} \quad (\text{B.6})$$

The first three  $d_n$ 's are given by  $\alpha_0 d_1 + \beta_0 d_0 = 0$  and  $d_{-1} = 0$ . Eq.(B.3), Eq.(B.5) and Eq.(B.6) tells us the following boundary condition

$$F'(0) = 0. \quad (\text{B.7})$$

We rewrite Eq.(B.5) as

$$d_{n+1} + A_n d_n + B_n d_{n-1} = 0, \quad (\text{B.8})$$

where  $A_n$  and  $B_n$  have asymptotic expansions of the form

$$\begin{cases} A_n = \frac{\beta_n}{\alpha_n} \sim \sum_{j=0}^{\infty} \frac{a_j}{n^j} \\ B_n = \frac{\gamma_n}{\alpha_n} \sim \sum_{j=0}^{\infty} \frac{b_j}{n^j} \end{cases} \quad (\text{B.9})$$

with

$$\begin{cases} a_0 = 0, & a_1 = -\lambda_{g,4}, & a_2 = \frac{\lambda_{g,4}}{2} \left( \Delta + 1 + \frac{\lambda_{g,4}}{2} \right) \\ b_0 = -1, & b_1 = 2 + \lambda_{g,4}, & b_2 = \frac{1}{4} (\lambda_{g,4} + \Delta)^2 + 2 + \lambda_{g,4} \end{cases} \quad (\text{B.10})$$

The radius of convergence,  $\rho$ , satisfies characteristic equation associated with Eq.(B.8) [49–51] :

$$\rho^2 + a_0\rho + b_0 = \rho^2 - 1 = 0, \quad (\text{B.11})$$

whose roots are given by

$$\rho_1 = 1 \quad \rho_2 = -1 \quad (\text{B.12})$$

So for a three-term recurrence relation in Eq.(B.5), the radius of convergence is 1 for all two cases. Since the solutions should converge at the horizon,  $y(z)$  should be convergent at  $|z| \leq 1$ . According to Pincherle's Theorem [52], we have a convergent solution of  $y(z)$  at  $|z| = 1$  if only if the three term recurrence relation Eq.(B.5) has a minimal solution. Since we have two different roots  $\rho_i$ 's, so Eq.(B.8) has two linearly independent solutions  $d_1(n)$ ,  $d_2(n)$ . One can show that [52] for large  $n$ ,

$$d_i(n) \sim \rho_i^n n^{\alpha_i} \sum_{r=0}^{\infty} \frac{\tau_i(r)}{n^r}, \quad i = 1, 2, 3 \quad (\text{B.13})$$

with

$$\alpha_i = \frac{a_1\rho_i + b_1}{a_0\rho_i + 2b_0}, \quad i = 1, 2 \quad (\text{B.14})$$

and  $\tau_i(0) = 1$ . In particular, we obtain

$$\tau_i(1) = \frac{-2\rho_i^2\alpha_i(\alpha_i - 1) - \rho_i(a_2 + \rho_i a_1 + \alpha_i(\alpha_i - 1)a_0/2) - b_2}{2\rho_i^2(\alpha_i - 1) + \rho_i(a_1 + (\rho_i - 1)a_0) + b_1}, \quad i = 1, 2 \quad (\text{B.15})$$

Substituting Eq.(B.12) and Eq.(B.10) into Eq.(B.13)–Eq.(B.15), we obtain

$$\begin{cases} d_1(n) \sim n^{-1} \left( 1 + \frac{\Delta^2 + 4\Delta\lambda_{g,4} + 2(\lambda_{g,4}^2 + \lambda_{g,4} + 12)}{8n} \right) \\ d_2(n) \sim (-1)^n n^{-1-\lambda_{g,4}} \left( 1 + \frac{\lambda_{g,4}^2 + \frac{11}{4}\lambda_{g,4} + \frac{\Delta^2}{8} + 3}{n} \right) \end{cases} \quad (\text{B.16})$$

Since  $\lambda_{g,4} > 0$ ,

$$\lim_{n \rightarrow \infty} \frac{d_2(n)}{d_1(n)} = 0. \quad (\text{B.17})$$

So  $d_2(n)$  is a minimal solution. Also,

$$\begin{cases} \sum |d_1(n)| \sim \sum \frac{1}{n} \rightarrow \infty \\ \sum |d_2(n)| \sim \sum n^{-1-\lambda_{g,4}} < \infty \end{cases} \quad (\text{B.18})$$

Therefore,  $y(z) = \sum_{n=0}^{\infty} d_n x^n$  is convergent at  $x = 1$  if only if  $d_n$  is a minimal solution. Eq.(A.13) with  $\delta_2 = \delta_3 = \dots = \delta_N = 0$  becomes a polynomial of degree  $N$  with respect to  $\lambda_{g,4}$ . Put Eq.(B.6) into Eq.(A.13) where  $\delta_i = 0$  at  $i \in \{2, 3, \dots, N\}$  and we choose  $N = 15$

For algorithm to find  $\lambda_{g,4}$  for a given  $\Delta$ ,

1. Choose an  $N$ .
2. Put Eq.(B.6) into Eq.(A.13).
3. Define a function returning the determinant of system Eq.(A.13).
4. Find the roots of interest of this function.
5. Increase  $N$  until those roots become constant to within the desired precision [10].

We use Mathematica to compute the determinants to locate their roots. We are only interested in smallest positive real roots of  $\lambda_{g,4}$ . For computation of roots, we choose  $N = 15$ .

For the smallest value of  $\lambda_{g,4}$ , we can find an approximate fitting function that is given by

$$\lambda_{g,4} \approx 0.59 (\Delta - 1)^{1/2} \left( \Delta^{0.7} + \left( \frac{1.61\Delta + 0.61}{\Delta + 1.42} \right)^5 \right) \quad (\text{B.19})$$

We calculated 121 different values of  $\lambda_{g,4}$ 's at various  $\Delta$  and the result is the pink colored dots in Fig. 10(a). These data fits well by above formula. The log-log plot of Fig. 10(b) shows that the exponent of  $(\Delta - 1)$  is  $1/2$  with high precision.

The authors of ref[56] got  $\lambda_{g,4}$ 's by using variational method using the fact that the eigenvalue  $\lambda_{g,4}$  minimizes the expression

$$\lambda_{g,4}^2 = \frac{\int_0^1 dz z^{2\Delta-3} \left( (1-z^4) [F'(z)]^2 + \Delta^2 z^2 [F(z)]^2 \right)}{\int_0^1 dz z^{2\Delta-3} \frac{1-z^2}{1+z^2} [F(z)]^2} \quad (\text{B.20})$$

for  $\Delta > 1$ . This integral does not converge at  $\Delta = 1$  because of  $\ln(z)$ . The trial function used is  $F(z) = 1 - \alpha z^3$  where  $\alpha$  is the variational parameter. The authors of ref. [56] got the value of  $\lambda_{1,4}$  by variational method. In Fig. 10(a) we denoted their result by the green dots and ours by the blue dots. The differences are appreciable at  $\Delta > 1.8$ . Our results are consistently lower.

The critical temperature which is given by  $T_c = \frac{1}{\pi} r_c = \frac{1}{\pi} \left( \frac{\rho}{\lambda_4} \right)^{\frac{1}{3}}$  which can be calculated by Eq.(B.19) and the Fig. 11 demonstrate the result. Notice that  $T_c$  is divergent at  $\Delta = 1$  and it is a monotonically decreasing function of  $\Delta$ .

### B.1.2 The analytic solution of $g \frac{\langle \mathcal{O}_\Delta \rangle}{T_c^\Delta}$

Substituting Eq.(B.3) into Eq.(2.3), the field equation  $\Phi$  becomes

$$\frac{d^2\Phi}{dx^2} = \frac{g^2 \langle \mathcal{O}_\Delta \rangle^2}{4r_h^{2\Delta}} \frac{x^{\Delta-2} F^2(x)}{1-x^2} \Phi \quad (\text{B.21})$$

where  $\frac{g^2 \langle \mathcal{O}_\Delta \rangle^2}{4r_h^{2\Delta}}$  is small because of  $T \approx T_c$ . The above equation has the expansion around Eq.(B.1) with small correction:

$$\frac{\Phi}{r_h} = \lambda_4(1-x) + \frac{g^2 \langle \mathcal{O}_\Delta \rangle^2}{4r_h^{2\Delta}} \chi_1(z) \quad (\text{B.22})$$

We have  $\chi_1(1) = \chi_1'(1) = 0$  due to the boundary conditions  $\Phi(1) = 0$ . Taking derivative of Eq.(B.22) twice with respect to  $x$  and using the result in Eq.(B.21),

$$\chi_1'' = \frac{x^{\Delta-2} F^2(z)}{1-x^2} \left\{ \lambda_4(1-x) + \frac{g^2 \langle \mathcal{O}_\Delta \rangle^2}{4r_h^{2\Delta}} \chi_1 \right\} \approx \frac{\lambda_4 x^{\Delta-2} F^2(z)}{1+x}. \quad (\text{B.23})$$

Integrating Eq.(B.23) gives us

$$\chi_1'(0) = -\lambda_4 \mathcal{C}_4 \quad \text{for } \mathcal{C}_4 = \int_0^1 dx \frac{x^{\Delta-2} F^2(x)}{1+x} \quad (\text{B.24})$$

Eq.(B.3) with Eq.(B.6) shows

$$F(z) = (1+x)^{-\lambda_{g,4}/2} y(x) \approx (1+x)^{-\lambda_{g,4}/2} \sum_{n=0}^1 d_n x^n \quad (\text{B.25})$$

Here, we ignore  $d_n x^n$  terms if  $n \geq 2$  because  $0 < |d_n| \ll 1$  numerically and  $y(x)$  converges at  $0 < x \leq 1$ . Put Eq.(B.25) into Eq.(B.24) and we have

$$\begin{aligned} \mathcal{C}_4 = & \frac{16\Delta(\Delta^2-1) {}_2F_1(1, \lambda_{g,4}+1; \Delta; \frac{1}{2})}{(\Delta-1)^2 \Delta(\Delta+1) 2^{5+\lambda_{g,4}}} \\ & + \frac{\lambda_{g,4}(-2\Delta+\lambda_{g,4}+2) (\Delta\lambda_{g,4}(-2\Delta+\lambda_{g,4}+2) {}_2F_1(1, \lambda_{g,4}+1; \Delta+2; \frac{1}{2}) - 8(\Delta^2-1) {}_2F_1(1, \lambda_{g,4}+1; \Delta+1; \frac{1}{2}))}{2^{5+\lambda_{g,4}} \Delta(\Delta+1)(\Delta-1)^2} \end{aligned} \quad (\text{B.26})$$

at  $\Delta > 1$ .

We can calculate the numerical value of  $\mathcal{C}_4$  by putting Eq.(B.19) into Eq.(B.26). We calculated 121 different values of  $\mathcal{C}_4$ 's at various  $\Delta$ , which is drawn as dots in Fig. 12. Then we tried to find an approximate fitting function. The result is given as follows,

$$\mathcal{C}_4 \approx \frac{16(\Delta^5 - 6.8\Delta^4 + 21.1\Delta^3 - 32.15\Delta^2 + 28.21\Delta - 6.26)^{-1}}{\pi(\Delta-1)} \quad (\text{B.27})$$

The Fig. 12 shows how the data fits by above formula. It is important to note that the integral for  $\mathcal{C}_4$  in Eq.(B.24) diverges at  $\Delta = 1$ . From Eq.(B.22) and Eq.(2.4), we have

$$\frac{\rho}{r_h^3} = \lambda_4 \left( 1 + \frac{\mathcal{C}_4 g^2 \langle \mathcal{O}_\Delta \rangle^2}{4r_h^{2\Delta}} \right) \quad (\text{B.28})$$

Putting  $T = \frac{1}{\pi} r_h$  with  $\lambda_4 = \frac{\rho}{r_h^3}$  into Eq.(B.28), we obtain the condensate near  $T_c$ :

$$g \frac{\langle \mathcal{O}_\Delta \rangle}{T_c^\Delta} \approx \mathcal{M}_4 \sqrt{1 - \frac{T}{T_c}} \quad \text{for } \mathcal{M}_4 = 2\pi^\Delta \sqrt{\frac{3}{\mathcal{C}_4}}, \quad (\text{B.29})$$

and the plot is in the FIG. 13.

## B.2 Condensate at near the zero temperature

### B.2.1 Analytic calculation of $g^{\frac{1}{\Delta}} \frac{\langle \mathcal{O}_\Delta \rangle^{\frac{1}{\Delta}}}{T_c}$ at $1 < \Delta < 4$

The dominant contribution comes from the neighborhood of the boundary  $z = 0$ . So near the  $T = 0$  we can simplify two coupled equations Eq.(2.3) and Eq.(2.3) with Eq.(B.3) by letting  $z \rightarrow 0$ :

$$\frac{d^2 F}{dz^2} + \frac{2\Delta - 3}{z} \frac{dF}{dz} + \frac{g^2 \Phi^2}{r_h^2} F = 0 \quad (\text{B.30a})$$

$$\frac{d^2 \Phi}{dx^2} - \frac{g^2 \langle \mathcal{O}_\Delta \rangle^2}{4r_h^{2\Delta}} x^{\Delta-2} F^2 \Phi = 0 \quad (\text{B.30b})$$

where  $x = z^2$ . Also, we use a boundary condition at the horizon, and Eq.(2.3) with Eq.(B.3) is rewritten as

$$-\frac{d^2 F}{dz^2} + \left( \frac{4}{z(1-z^4)} - \frac{2\Delta+1}{z} \right) \frac{dF}{dz} + \left( \frac{\Delta^2 z^2}{1-z^4} - \frac{g^2 \Phi^2}{r_h^2 (1-z^4)^2} \right) F = 0. \quad (\text{B.31})$$

It provides us the following boundary condition at the horizon with Eq.(2.3),  $\Phi(1) = 0$  and  $\Psi(1) < \infty$ :

$$4F'(1) + \Delta^2 F(1) = 0 \quad (\text{B.32})$$

By multiplying  $z$  to the eq. (B.31) and then taking the limit of  $z \rightarrow 0$ , we get  $F'(0) = 0$ . Note that  $F(0) = 1$  should be considered as the normalization condition of  $\langle \mathcal{O}_\Delta \rangle$  rather than as a boundary condition. Also for canonical system, we regard the  $\frac{d\Phi(0)}{dx} = -\frac{\rho}{r_h^2}$  as BC and  $\Phi(0) = \mu$  is not a BC but a value that should be determined by  $\rho$  from the horizon regularity condition  $\Phi(1) = 0$ . In Grand canonical system  $\Phi(0) = \mu$  is the boundary condition and  $\rho$  should be determined from it by the  $\Phi(1) = 0$ . Here we consider  $\rho$  as the given parameter.

If we introduce  $b$  by for  $b^\Delta = \frac{g \langle \mathcal{O}_\Delta \rangle}{\Delta r_h^\Delta}$ , the solution to Eq.(B.30b) for  $\Phi$  with  $F \approx 1$  is

$$\Phi(z) = \mathcal{A} r_h b z K_{\frac{1}{\Delta}}(b^\Delta z^\Delta) \quad (\text{B.33})$$

At the horizon  $\Phi(1) \propto \exp(-b^\Delta) \rightarrow 0$  because  $b \rightarrow \infty$  as  $r_h \rightarrow 0$ , which takes care the boundary condition  $\Phi(1) = 0$ . Substituting Eq.(B.33) into Eq.(B.30a),  $F$  becomes

$$\frac{d^2 F}{dz^2} + \frac{2\Delta - 3}{z} \frac{dF}{dz} + g^2 b^2 \mathcal{A}^2 z^2 \left( K_{\frac{1}{\Delta}}(b^\Delta z^\Delta) \right)^2 F = 0 \quad (\text{B.34})$$

$F(z)$  can be obtained iteratively starting from  $F = 1$ . The result is

$$F(z) = 1 - g^2 b^2 \mathcal{A}^2 \int_0^z dz z^{3-2\Delta} \int_0^z d\tilde{z} \tilde{z}^{2\Delta-1} \left( K_{\frac{1}{\Delta}}(b^\Delta \tilde{z}^\Delta) \right)^2 \quad (\text{B.35a})$$

$$F'(z) = -g^2 b^2 \mathcal{A}^2 z^{3-2\Delta} \int_0^z d\tilde{z} \tilde{z}^{2\Delta-1} \left( K_{\frac{1}{\Delta}}(b^\Delta \tilde{z}^\Delta) \right)^2. \quad (\text{B.35b})$$

with the boundary condition  $F'(0) = 0$  and normalized  $F(0) = 1$ . Applying Eq.(B.32), we have

$$g^2 \mathcal{A}^2 = \frac{\Delta^2 b^2}{4F'_\Delta(b) + \Delta^2 F_\Delta(b)} \quad (\text{B.36})$$

where

$$F_\Delta(b) = \int_0^b dz z^{3-2\Delta} \int_0^z d\tilde{z} \tilde{z}^{2\Delta-1} \left( K_{\frac{1}{\Delta}}(\tilde{z}^\Delta) \right)^2 \quad (\text{B.37a})$$

$$F'_\Delta(b) = b^{4-2\Delta} \int_0^b dz z^{2\Delta-1} \left( K_{\frac{1}{\Delta}}(z^\Delta) \right)^2 \quad (\text{B.37b})$$

Letting  $x = z^\Delta$ , Eq.(B.37b) is simplified as

$$F'_\Delta(b) = \frac{b^{4-2\Delta}}{\Delta} \int_0^{b^\Delta} dx x \left( K_{\frac{1}{\Delta}}(x) \right)^2 = \frac{b^{4-2\Delta}}{\Delta} \int_0^\infty dx x \left( K_{\frac{1}{\Delta}}(x) \right)^2. \quad (\text{B.38})$$

Using Eq.(A.47), Eq.(B.38) becomes

$$F'_\Delta(b) = \frac{\pi b^{4-2\Delta}}{2\Delta^2} \csc\left(\frac{\pi}{\Delta}\right) \quad (\text{B.39})$$

Letting  $x = \tilde{z}^\Delta$ , Eq.(B.37a) is also simplified as

$$F_\Delta(b) = \frac{1}{\Delta} \int_0^b dz z^{3-2\Delta} \int_0^{z^\Delta} dx x \left( K_{\frac{1}{\Delta}}(x) \right)^2 \quad (\text{B.40})$$

As we apply Eq.(A.47), Eq.(A.50) and Eq.(A.51) into Eq.(B.40), we obtain

$$\begin{aligned} F_\Delta(b) &= \frac{\pi b^{4-2\Delta}}{4\Delta^2(2-\Delta)} \csc\left(\frac{\pi}{\Delta}\right) - \frac{\pi \epsilon^{4-2\Delta}}{4\Delta^2(2-\Delta)} \csc\left(\frac{\pi}{\Delta}\right) \\ &+ \frac{1}{2\Delta^2} \lim_{\epsilon \rightarrow 0} \int_{\epsilon^\Delta}^{b^\Delta} dx x^{\frac{4-\Delta}{\Delta}} K_{\frac{1}{\Delta}}(x)^2 - \frac{1}{2\Delta^2} \lim_{\epsilon \rightarrow 0} \int_{\epsilon^\Delta}^{b^\Delta} dx x^{\frac{4-\Delta}{\Delta}} K_{\frac{1}{\Delta}-1}(x) K_{\frac{1}{\Delta}+1}(x) \\ &\approx \frac{\pi b^{4-2\Delta}}{4\Delta^2(2-\Delta)} \csc\left(\frac{\pi}{\Delta}\right) - \frac{\pi \epsilon^{4-2\Delta}}{4\Delta^2(2-\Delta)} \csc\left(\frac{\pi}{\Delta}\right) \\ &+ \frac{1}{2\Delta^2} \int_0^\infty dx x^{\frac{4-\Delta}{\Delta}} K_{\frac{1}{\Delta}}(x)^2 - \frac{1}{2\Delta^2} \lim_{\epsilon \rightarrow 0} \int_{\epsilon^\Delta}^{b^\Delta} dx x^{\frac{4-\Delta}{\Delta}} K_{\frac{1}{\Delta}-1}(x) K_{\frac{1}{\Delta}+1}(x) \\ &= \frac{\pi b^{4-2\Delta}}{4\Delta^2(2-\Delta)} \csc\left(\frac{\pi}{\Delta}\right) - \frac{\pi \epsilon^{4-2\Delta}}{4\Delta^2(2-\Delta)} \csc\left(\frac{\pi}{\Delta}\right) \\ &+ \frac{\sqrt{\pi}}{8\Delta^2} \frac{\Gamma(1/\Delta)\Gamma(2/\Delta)\Gamma(3/\Delta)}{\Gamma(1/2+2/\Delta)} - \frac{1}{2\Delta^2} \lim_{\epsilon \rightarrow 0} \int_{\epsilon^\Delta}^{b^\Delta} dx x^{\frac{4-\Delta}{\Delta}} K_{\frac{1}{\Delta}-1}(x) K_{\frac{1}{\Delta}+1}(x) \end{aligned} \quad (\text{B.41})$$

here, we introduce small  $\epsilon$ , and take zero at the end of calculations. After some long but simple calculations using the properties Eq.(A.53), Eq.(A.54) and Eq.(A.55), an integral in Eq.(B.41) is shows

$$-\frac{1}{2\Delta^2} \lim_{\epsilon \rightarrow 0} \int_{\epsilon\Delta}^{b\Delta} dx x^{\frac{4-\Delta}{\Delta}} K_{\frac{1}{\Delta}-1}(x) K_{\frac{1}{\Delta}+1}(x) = \frac{\sqrt{\pi}\Gamma(\frac{1}{\Delta})\Gamma(\frac{2}{\Delta})\Gamma(\frac{3}{\Delta})}{4\Delta^2(\Delta-2)\Gamma(\frac{1}{2}+\frac{2}{\Delta})} + \frac{\pi\epsilon^{4-2\Delta}}{4\Delta^2(2-\Delta)} \csc\left(\frac{\pi}{2\Delta}\right) \quad (\text{B.42})$$

with  $b \rightarrow \infty$ . Substitute Eq.(B.42) into Eq.(B.41), and we have

$$F_\Delta(b) = \frac{\pi b^{4-2\Delta}}{4\Delta^2(2-\Delta)} \csc\left(\frac{\pi}{\Delta}\right) - \frac{\sqrt{\pi}\Gamma(-1+\frac{2}{\Delta})\Gamma(\frac{1}{\Delta})\Gamma(\frac{3}{\Delta})}{8\Delta^2\Gamma(\frac{1}{2}+\frac{2}{\Delta})} \quad (\text{B.43})$$

Putting Eq.(B.39) and Eq.(B.43) into Eq.(B.36), we have

$$g^2 \mathcal{A}^2 = \frac{b^2}{\frac{\pi(4-\Delta)^2 \csc(\frac{\pi}{\Delta})}{4\Delta^4(2-\Delta)} b^{4-2\Delta} - \frac{\sqrt{\pi}\Gamma(\frac{1}{\Delta})\Gamma(\frac{3}{\Delta})\Gamma(-1+\frac{2}{\Delta})}{8\Delta^2\Gamma(\frac{1}{2}+\frac{2}{\Delta})}} \quad (\text{B.44})$$

Apply Eq.(A.51) into Eq.(B.33) using Eq.(2.4), we deduce

$$\frac{\rho}{r_h^3} = -\frac{\Gamma(-\frac{1}{\Delta})}{2^{1+\frac{1}{\Delta}}} \mathcal{A} b^2 \quad (\text{B.45})$$

As we combine  $T_c = \frac{1}{\pi} r_c = \frac{1}{\pi} \left(\frac{\rho}{\lambda_4}\right)^{\frac{1}{3}}$ , Eq.(B.19), Eq.(B.44) and Eq.(B.45) with  $b = \left(\frac{g\langle\mathcal{O}_\Delta\rangle}{\Delta r_h^{\frac{\Delta}{2}}}\right)^{\frac{1}{\Delta}}$  in Eq.(B.33) in the form of  $X$ ; here,  $X := \langle\mathcal{O}_\Delta\rangle^{\frac{1}{\Delta}}/T_c$  for simple notation, we describec the condensate at  $T \approx 0$ :

$$X^6 = G_4^6 (\alpha_4 + \beta_4 \tau_4^{4-2\Delta} X^{4-2\Delta}) \quad (\text{B.46})$$

$$\begin{aligned} \text{where } G_4 &= \pi \Delta^{1/\Delta} \left( \frac{-2^{1+\frac{1}{\Delta}} \lambda_{g,4}}{\Gamma(-\frac{1}{\Delta})} \right)^{\frac{1}{3}} \\ \alpha_4 &= -\frac{\sqrt{\pi}\Gamma(\frac{2-\Delta}{\Delta})\Gamma(\frac{1}{\Delta})\Gamma(\frac{3}{\Delta})}{8\Delta^2\Gamma(\frac{4+\Delta}{2\Delta})} \\ \beta_4 &= \frac{\nu\pi(4-\Delta)^2 \csc(\nu\pi)}{4\Delta^3(2-\Delta)} \end{aligned} \quad (\text{B.47})$$

with  $\nu = \frac{1}{\Delta}$  and  $\tau_4 = \frac{1}{\pi\Delta^{1/\Delta}} \frac{T_c}{T}$ .

### B.2.2 Analytic calculation of $g^{\frac{1}{\Delta}} \frac{\langle\mathcal{O}_\Delta\rangle^{\frac{1}{\Delta}}}{T_c}$ at $\Delta = 2$

$\alpha_4$  and  $\beta_4$  in Eq.(B.47) have series expansions at  $\Delta = 2$ :

$$\alpha_4 = \frac{\pi \csc(\frac{\pi}{2})}{4^2(\Delta-2)} + \frac{2\pi \csc(\frac{\pi}{2})(4-4\log(4)-6\psi(3/2)-2\psi(1/2))}{4^4} + \mathcal{O}(\Delta-2) \quad (\text{B.48})$$

$$\beta_4 = -\frac{\pi \csc(\frac{\pi}{2})}{4^2(\Delta-2)} + \frac{2\pi \csc(\frac{\pi}{2})(24+2\pi \cot(\frac{\pi}{2}))}{4^4} + \mathcal{O}(\Delta-2). \quad (\text{B.49})$$

As Eq.(B.48) and Eq.(B.49) are substituted into Eq.(B.46) with taking the limit  $\Delta \rightarrow 2$ , we obtain

$$X^6 = G_4^6 \left( \rho_4 + \frac{\sigma_4}{2} \left( \frac{1 - \tau_4^{4-2\Delta} X^{4-2\Delta}}{\Delta - 2} \right) \right) \quad (\text{B.50})$$

where

$$\begin{aligned} \sigma_4 &= \frac{\pi \csc\left(\frac{\pi}{2}\right)}{8} \\ \rho_4 &= \frac{\sigma_4}{4} \left( 28 - 4 \ln(4) + 2\pi \cot\left(\frac{\pi}{2}\right) - 6\psi(3/2) - 2\psi(1/2) \right) \\ &= \frac{\sigma_4}{4} \left( 4 - \pi \cot\left(\frac{\pi}{2}\right) - \ln(4) - 2\psi(1/2) \right) \end{aligned}$$

By using L'Hopital's rule, Eq.(B.50) becomes

$$\begin{aligned} X^6 &= G_4^6 \left( \rho_4 - \frac{\sigma_4}{2} \frac{\partial}{\partial \Delta} (\tau_4^{4-2\Delta} X^{4-2\Delta}) \right) \\ &= G_4^6 (\rho_4 + \sigma_4 \ln(\tau_4 X)) \end{aligned} \quad (\text{B.51})$$

Fig. 21 (b) tells us that  $X \sim \ln(T_c/T)^{1/6}$  for low temperature; Numerical result tells us that  $X^6 - \log(T/T_c)$  plot demonstrates the validity of our result with high precision:  $X$  is numerically

$$X \approx 4.9 \left( 1 + 0.57 \ln\left(\frac{T_c}{T}\right) \right)^{1/6} \quad (\text{B.52})$$

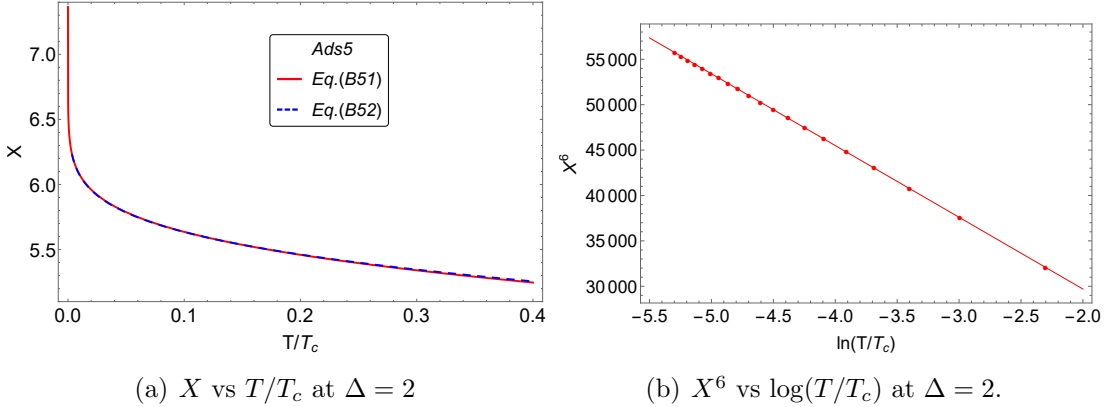


**Figure 21:** (a)  $X$  vs  $T/T_c$ : red colored curves for  $X$  is a plot of Eq.(B.51). And blue curves is a plot of Eq.(B.52). These two curves are almost identical for low temperature. (b)  $X^6$  vs  $\log(T/T_c)$  at  $\Delta = 2$ : The slope of red dotted line for  $X^6$  is  $-7900$ .

## References

- [1] J. M. Maldacena, *The Large  $N$  limit of superconformal field theories and supergravity*, *Int.J.Theor.Phys.* **38** (1999) 1113–1133, [[hep-th/9711200](#)].

- [2] E. Witten, *Anti-de Sitter space and holography*, *Adv. Theor. Math. Phys.* **2** (1998) 253–291, [[hep-th/9802150](#)].
- [3] S. S. Gubser, I. R. Klebanov and A. M. Polyakov, *Gauge theory correlators from noncritical string theory*, *Phys. Lett.* **B428** (1998) 105–114, [[hep-th/9802109](#)].
- [4] S. A. Hartnoll, C. P. Herzog and G. T. Horowitz, *Building a holographic superconductor*, *Physical Review Letters* **101** (2008) 031601.
- [5] S. S. Gubser, *Breaking an Abelian gauge symmetry near a black hole horizon*, *Phys.Rev.* **D78** (2008) 065034, [[0801.2977](#)].
- [6] S. A. Hartnoll, A. Lucas and S. Sachdev, *Holographic quantum matter*, [1612.07324](#).
- [7] G. T. Horowitz and M. M. Roberts, *Holographic superconductors with various condensates*, *Physical Review D* **78** (2008) 126008.
- [8] G. Siopsis and J. Therrien, *Analytic calculation of properties of holographic superconductors*, *Journal of High Energy Physics* **2010** (2010) 1–18.
- [9] F. Denef and S. A. Hartnoll, *Landscape of superconducting membranes*, *Physical Review D* **79** (2009) 126008.
- [10] E. W. Leaver, *Quasinormal modes of reissner-nordström black holes*, *Physical Review D* **41** (1990) 2986.
- [11] C. P. Herzog, *Analytic holographic superconductor*, *Physical Review D* **81** (2010) 126009.
- [12] X. Qiao, D. Wang, L. OuYang, M. Wang, Q. Pan and J. Jing, *An analytic study on the excited states of holographic superconductors*, *Physics Letters B* **811** (2020) 135864.
- [13] E. Mefford and G. T. Horowitz, *Simple holographic insulator*, *Physical Review D* **90** (2014) 084042.
- [14] G. T. Horowitz, *Introduction to holographic superconductors*, in *From gravity to thermal gauge theories: the AdS/CFT correspondence*, pp. 313–347. Springer, 2011.
- [15] R. Cai, L. Li, L. Li and R. Yang, *Introduction to holographic superconductor models*, *Science China Physics, Mechanics & Astronomy* **58** (2015) 1–46.
- [16] X.-H. Ge, B. Wang, S.-F. Wu and G.-H. Yang, *Analytical study on holographic superconductors in external magnetic field*, *Journal of High Energy Physics* **2010** (2010) 1–19.
- [17] S. Gangopadhyay and D. Roychowdhury, *Analytic study of properties of holographic p-wave superconductors*, *Journal of High Energy Physics* **2012** (2012) 1–12.
- [18] Q. Pan and B. Wang, *General holographic superconductor models with gauss–bonnet corrections*, *Physics Letters B* **693** (2010) 159–165.
- [19] R.-G. Cai, H.-F. Li and H.-Q. Zhang, *Analytical studies on holographic insulator/superconductor phase transitions*, *Physical Review D* **83** (2011) 126007.
- [20] J. Jing, Q. Pan and S. Chen, *Holographic superconductors with power-maxwell field*, *Journal of High Energy Physics* **2011** (2011) 1–12.

- [21] D. Roychowdhury, *Effect of external magnetic field on holographic superconductors in presence of nonlinear corrections*, *Physical Review D* **86** (2012) 106009.
- [22] S. Gangopadhyay and D. Roychowdhury, *Analytic study of gauss-bonnet holographic superconductors in born-infeld electrodynamics*, *Journal of High Energy Physics* **2012** (2012) 1–10.
- [23] H.-F. Li, R.-G. Cai and H.-Q. Zhang, *Analytical studies on holographic superconductors in gauss-bonnet gravity*, *Journal of High Energy Physics* **2011** (2011) 1–14.
- [24] Q. Pan, J. Jing and B. Wang, *Analytical investigation of the phase transition between holographic insulator and superconductor in gauss-bonnet gravity*, *Journal of High Energy Physics* **2011** (2011) 1–17.
- [25] H.-B. Zeng, X. Gao, Y. Jiang and H.-S. Zong, *Analytical computation of critical exponents in several holographic superconductors*, *Journal of High Energy Physics* **2011** (2011) 1–17.
- [26] R. Flauger, E. Pajer and S. Papanikolaou, *Striped holographic superconductor*, *Physical Review D* **83** (2011) 064009.
- [27] Z. Zhao, Q. Pan, S. Chen and J. Jing, *Notes on holographic superconductor models with the nonlinear electrodynamics*, *Nuclear Physics B* **871** (2013) 98–110.
- [28] Y. Liu, Q. Pan and B. Wang, *Holographic superconductor developed in btz black hole background with backreactions*, *Physics Letters B* **702** (2011) 94–99.
- [29] Z. Zhao, Q. Pan and J. Jing, *Holographic insulator/superconductor phase transition with weyl corrections*, *Physics Letters B* **719** (2013) 440–447.
- [30] D. Roychowdhury, *Ads/cft superconductors with power maxwell electrodynamics: reminiscent of the meissner effect*, *Physics Letters B* **718** (2013) 1089–1094.
- [31] S. Kanno, *A note on gauss–bonnet holographic superconductors*, *Classical and Quantum Gravity* **28** (2011) 127001.
- [32] Y. Peng, Q. Pan and B. Wang, *Various types of phase transitions in the ads soliton background*, *Physics Letters B* **699** (2011) 383–387.
- [33] Q. Pan, J. Jing, B. Wang and S. Chen, *Analytical study on holographic superconductors with backreactions*, *Journal of High Energy Physics* **2012** (2012) 1–12.
- [34] R. Banerjee, S. Gangopadhyay, D. Roychowdhury and A. Lala, *Holographic s-wave condensate with nonlinear electrodynamics: A nontrivial boundary value problem*, *Physical Review D* **87** (2013) 104001.
- [35] W. Yao and J. Jing, *Analytical study on holographic superconductors for born-infeld electrodynamics in gauss-bonnet gravity with backreactions*, *Journal of High Energy Physics* **2013** (2013) 1–16.
- [36] J.-W. Lu, Y.-B. Wu, P. Qian, Y.-Y. Zhao, X. Zhang and N. Zhang, *Lifshitz scaling effects on holographic superconductors*, *Nuclear Physics B* **887** (2014) 112–135.
- [37] A. Sheykhi, H. R. Salahi and A. Montakhab, *Analytical and numerical study of*

- gauss-bonnet holographic superconductors with power-maxwell field*, *Journal of High Energy Physics* **2016** (2016) 1–17.
- [38] D. Ghorai and S. Gangopadhyay, *Higher dimensional holographic superconductors in born–infeld electrodynamics with back-reaction*, *The European Physical Journal C* **76** (2016) 1–12.
- [39] A. Sheykhi and F. Shaker, *Analytical study of holographic superconductor in born–infeld electrodynamics with backreaction*, *Physics Letters B* **754** (2016) 281–287.
- [40] C. Lai, Q. Pan, J. Jing and Y. Wang, *On analytical study of holographic superconductors with born–infeld electrodynamics*, *Physics Letters B* **749** (2015) 437–442.
- [41] Y. Liu, Q. Pan, B. Wang and R.-G. Cai, *Dynamical perturbations and critical phenomena in gauss–bonnet ads black holes*, *Physics Letters B* **693** (2010) 343–350.
- [42] J. Erdmenger, X.-H. Ge and D.-W. Pang, *Striped phases in the holographic insulator/superconductor transition*, *Journal of High Energy Physics* **2013** (2013) 1–29.
- [43] X.-M. Kuang, E. Papantonopoulos, G. Siopsis and B. Wang, *Building a holographic superconductor with higher-derivative couplings*, *Physical Review D* **88** (2013) 086008.
- [44] S. Gangopadhyay, *Holographic superconductors in born–infeld electrodynamics and external magnetic field*, *Modern Physics Letters A* **29** (2014) 1450088.
- [45] L. Zhang, Q. Pan and J. Jing, *Holographic p-wave superconductor models with weyl corrections*, *Physics Letters B* **743** (2015) 104–111.
- [46] R.-G. Cai, L. Li, H.-Q. Zhang and Y.-L. Zhang, *Magnetic field effect on the phase transition in ads soliton spacetime*, *Physical Review D* **84** (2011) 126008.
- [47] K.-Y. Kim and M. Taylor, *Holographic d-wave superconductors*, *Journal of High Energy Physics* **2013** (2013) 112.
- [48] W. Yao and J. Jing, *Holographic entanglement entropy in metal/superconductor phase transition with born–infeld electrodynamics*, *Nuclear Physics B* **889** (2014) 109–119.
- [49] L. M. Milne-Thomson, *The calculus of finite differences*. American Mathematical Soc., 2000.
- [50] O. Perron, *Über summengleichungen und poincarésche differenzgleichungen*, *Mathematische Annalen* **84** (1921) 1–15.
- [51] H. Poincare, *Sur les équations linéaires aux différentielles ordinaires et aux différences finies*, *American Journal of Mathematics* (1885) 203–258.
- [52] W. B. Jones and W. J. Thron, *Continued fractions: Analytic theory and applications*, vol. 11. Addison-Wesley Publishing Company, 1980.
- [53] I. S. Gradshteyn and I. M. Ryzhik, *Table of integrals, series, and products*. Academic press, 2014.
- [54] I. Thompson, *Nist handbook of mathematical functions, edited by frank wj olver, daniel w. lozier, ronald f. boisvert, charles w. clark*, 2011.

- [55] F. M. Arscott, S. Y. Slavyanov, D. Schmidt, G. Wolf, P. Maroni and A. Duval, *Heun's differential equations*. Clarendon Press, 1995.
- [56] G. Siopsis, J. Therrien and S. Musiri, *Holographic superconductors near the breitenlohner–freedman bound*, *Classical and Quantum Gravity* **29** (2012) 085007.